ISSN 1905-9094

GMSARN INTERNATIONAL JOURNAL

Vol. 8 No. 2
June 2014

Published by the

GREATER MEKONG SUBREGION ACADEMIC AND RESEARCH NETWORK
c/o Asian Institute of Technology
P.O. Box 4, Klong Luang, Pathumthani 12120, Thailand

GMSARN INTERNATIONAL JOURNAL

GMSARN MEMBERS

Asian Institute of Technology	P.O. Box 4, Klong Luang, Pathumthani 12120, Thailand. www.ait.asia
Guangxi University	100, Daxue Road, Nanning, Guangxi, CHINA www.gxu.edu.cn
Hanoi University of Science and Technology	No. 1, Daicoviet Street, Hanoi, Vietnam S.R. www.hust.edu.vn
Ho Chi Minh City University of Technology	268 Ly Thuong Kiet Street, District 10, Ho Chi Minh City, Vietnam. www.hcmut.edu.vn
Institute of Technology of Cambodia	BP 86 Blvd. Pochentong, Phnom Penh, Cambodia. www.itc.edu.kh
Khon Kaen University	123 Mittraparb Road, Amphur Muang, Khon Kaen, Thailand. www.kku.ac.th
Kunming University of Science and Technology	121 Street, Kunming P.O. 650093, Yunnan, China. www.kmust.edu.cn
Nakhon Phanom University	330 Apibanbuncha Road, Nai Muang Sub-District, Nakhon Phanom 48000, THAILAND www.npu.ac.th
National University of Laos	P.O. Box 3166, Vientiane Perfecture, Lao PDR. www.nuol.edu.la
Royal University of Phnom Penh	Russian Federation Blvd, PO Box 2640 Phnom Penh, Cambodia. www.rupp.edu.kh
Thammasat University	P.O. Box 22, Thamamasat Rangsit Post Office, Bangkok 12121, Thailand. www.tu.ac.th
Ubon Ratchathani University	85 Sathollmark Rd. Warinchamrap Ubon Ratchathani 34190, THAILAND www.ubu.ac.th
Yangon Technological University	Gyogone, Insein P.O. Yangon, Myanmar www.most.gov.mm/ytu/
Yunnan University	2 Cuihu Bei Road Kunming, 650091, Yunnan Province, China. www.ynu.edu.cn

ASSOCIATE MEMBER

Mekong River Commission	P.O. Box 6101, Unit 18 Ban Sithane Neua, Sikhottabong District, Vientiane 01000, LAO PDR www.mrcmekong.org

GMSARN
INTERNATIONAL JOURNAL

GREATER MEKONG SUBREGION ACADEMIC AND RESEARCH NETWORK (http://www.gmsarn.com)

The Greater Mekong Subregion (GMS) consists of Cambodia, China (Yunnan & Guangxi Provinces), Laos, Myanmar, Thailand and Vietnam.

The Greater Mekong Subregion Academic and Research Network (GMSARN) was founded followed an agreement among the founding GMS country institutions signed on 26 January 2001, based on resolutions reached at the Greater Mekong Subregional Development Workshop held in Bangkok, Thailand, on 10 - 11 November 1999. GMSARN was composed of eleven of the region's top-ranking academic and research institutions. GMSARN carries out activities in the following areas: human resources development, joint research, and dissemination of information and intellectual assets generated in the GMS. GMSARN seeks to ensure that the holistic intellectual knowledge and assets generated, developed and maintained are shared by organizations within the region. Primary emphasis is placed on complementary linkages between technological and socio-economic development issues. Currently, GMSARN is sponsored by Royal Thai Government.

The GMSARN current member institutions are the Asian Institute of Technology, Pathumthani, Thailand; Guangxi University, Guangxi Province, China; Hanoi University of Science and Technology, Hanoi, Vietnam; Ho Chi Minh City University of Technology, Ho Chi Minh City, Vietnam; The Institute of Technology of Cambodia, Phnom Penh, Cambodia; Khon Kaen University, Khon Kaen Province, Thailand; Kunming University of Science and Technology, Yunnan Province, China; Nakhon Phanom University, Nakon Phanom Province, Thailand; National University of Laos, Vientiane, Laos PDR; The Royal University of Phnom Penh, Phnom Penh, Cambodia; Thammasat University, Bangkok, Thailand; Ubon Ratchathani University, Ubon Ratchathani Province, Thailand; Yangon Technological University, Yangon, Myanmar; and Yunnan University, Yunnan Province, China and another associate member is Mekong River Commission, Vientiane, Laos PDR.

GMSARN International Journal

Volume 8, Number 2, June 2014

CONTENTS

Energy Potential of Biogas Production from Animal Manure in the Lao People's Democratic Republic

Dethanou Koumphonphakdi and Ratchaphon Suntivarakorn*

***Abstract*— *This paper presented a study of biogas production potential from animal manure in the Lao People Democratic Republic (Lao PDR). The data from four kinds of animal such as cow, buffalo, pig and chicken were surveyed and calculated in order to know the potential of biogas production. The feasibility study of biogas production from pig farm in a case study was also done in order to know the investment cost as the net present value (NPV), the internal rate of return (IRR), the payback period (PB) and the benefit cost ratio (B/C). From a study, it was found that the Lao P.D.R had 31,747,297 of all animals and the potential for biogas production was 807 million m^3/year, which can produce the electricity of 1,163 million kWh/year. The highest potential for biogas production are in Salavanh, Savannakhet and Champasak provinces, which had the potential to produce 162.96, 123.51, and 70.72 million m^3/year of biogas, respectively. In addition, from the feasibility study in a case study with 520 pigs, it was revealed that biogas production from pig manure was a high feasible project, which can produce biogas of 175.3 m^3/day or 245 kWh/day of electricity. The project cost is amount 174.70 million kip of investment for biogas production system. From the economic analysis of this study, it was found that the NPV was 144.77 million kip, the IRR was 22.96%, PB was 4.1 years and the B/C was 1.82. This project is suitable for investment and it can be a data base for set up the policy to promote the biogas production in the Lao PDR.*

***Keywords*— Energy potential, biogas, animal manure, feasibility study.**

1. INTRODUCTION

The Lao People's Democratic Republic (Lao P.D.R) has total population of 6.5 million people in year 2010, and the most of population about 80 percent were agriculture, especially rice farmer and rancher. Since the Lao P.D.R opened the country in 1986, it made the Lao P.D.R economic continuously grows up to now, and caused of energy consumption increasing. Although the Lao P.D.R is a country that can produce the power electricity from several large dams and sell the electricity to neighbor countries, there is a lack of domestic electrical energy at some time. Besides, the Lao government has the policy to increase an electrification rate up to 90 percent by 2020 [1], and has the policy to promote the use of renewable energy. However, the Lao P.D.R has insufficient information on the production of electricity from renewable energy sources, particularly the production of biogas from animal manure.

The objective of this work is to study an energy potential of biogas production from manure in the Lao People Democratic Republic (Lao P.D.R). The datum of four kinds of animals, consisting of cow, buffalo, pig and chicken were collected and investigated. Then, the biogas production potential will be calculated from animal manure. The case study of biogas production in pig farm will be studied to know the economic feasibility of biogas production project in Lao PDR.

Therefore, researchers are interested in study the potential of biogas production from animal manure to obtain the information and helpful guidelines for further alternative energy development in Lao PDR

2. RESEARCH METHOD

The research method was divided in to four main components, which are data collection, data analysis, economic analysis and data summary.

2.1 Data Collection

The data was collected from the Department of Livestock and Fisheries, Ministry of Agriculture and Forestry. The obtained information consists of

1) The number of animals and farm in nationwide, there are four kinds of animals consisting of cow, buffalo, pig and chicken.

2) The farm's location and name's farmer in the provinces.

In addition, the data for case study feasibility was also collected by interview with the staff working in the Animals Research Centre, the Pig and Poultry Breeding Station, Ministry of Agriculture and Forestry in Lao PDR.

2.2 Data Analysis

The data analysis was divided in two parts as follow:

1) In order to know the energy potential of biogas production. Four kind of animals manure such as cow, buffalo, pig and chicken were collected. The gathering of

Dethanou Koumphonphakdi was graduated from Department of Mechanical Engineering, Faculty of Engineering, Khon Kaen University, Thailand. Tel: +66 865265030; E-mail: dethanou@yahoo.com,

Ratchaphon Suntivarakorn (corresponding author) is the Head of Department of Mechanical Engineering, Faculty of Engineering, Khon Kaen University. Tel: + 66 819891983; Fax: +66 37347879; E-mail: ratchaphon@kku.ac.th.

each manure has the ratio of 50%, 50%, 80% and 90%, respectively [2].

2) From the case study, the amount of pig was analyzed to find the feasibility of the biogas production project. Four financial analyses were used to study the project feasibility, there were the net present value (NPV), the internal rate of return (IRR), the payback period (PB) and the benefit cost ratio (B/C).

2.3 Economic Analysis

The economic analysis of this project was considered by the four economic parameters as follow [3].

1) Net Present Value: NPV

The NPV is the difference between the net present value of income and expenses over the life of the project. NPV is an indicator of net benefit of the project as the equation below:

$$NPV = PVB - PVC \quad (1)$$

where the PVB is the present value of benefit and PVC is the present value of cost. If the NPV is more than 0 (zero), the benefit of project is more than the project cost. The project is high feasible for investment.

2) Internal Rate of Return : IRR

The IRR is the return from the investment. IRR is a rate that makes the present value of revenue equal to the initial investment of the project. IRR can be calculated by:

$$\sum_{t=1}^{n} \frac{R_t}{(1+k)^t} = I \quad (2)$$

where the Rt is Bt - Ct, Bt and Ct are the benefit and cost in the time during the project, k is the return of the project (IRR) and I is the initial cost . If the IRR is more than the discount rate, it can be acceptable for the project. The project will be rejectable when the IRR is less than or equal to the discount rate.

3) Payback Period: PB

The payback period is the duration (number of years) when the return is equal to investment. The PB can be calculated by

$$PB = \text{Initial Cost} / \text{Net Revenue} \quad (3)$$

If the project can be returned by short time, it is acceptable for the project.

4) Benefit Cost ratio: B/C

The B/C is a comparison between the present value of the return and the current cost of the investment and expenses. B/C can be calculated by:

$$B/C = \left(\sum_{t=0}^{n} \frac{B_t}{(1+i)^t}\right) / \left(\sum_{t=0}^{n} \frac{C_t}{(1+i)^t}\right) \quad (4)$$

If the B/C is more than 1, that means the return of project will be worth. However, if the value is less than 1, that means the returns from the project is not worth for investment.

2.4 Data Summary

To obtain the information in order to use and set up the policy for alternative energy promotion in Lao PDR, the energy production potential was divided by provinces and types of animal. The data from feasibility study was also summarized in this part.

3. THE ENERGY POTENTIAL OF BIOGAS PRODUCTION

From the data collection of animal farms, the Lao P.D.R has 17 provinces that having animal farms. The number of animal from four kinds of animals: cow, buffalo, pig and chicken were shown in Table 1.

Table 1. The amount of animals in Lao PDR [4] (1,000 unit)

Provinces	Cow	Buffalo	Pig	Chicken	Total
Phongsaly	23	37	170	554	785
Louang namtha	20	17	88	458	584
Oudomxay	49	44	140	1,476	1,703
Bokeo	54	24	62	402	542
Louang phabang	79	63	179	1,869	2,190
Huaphan	72	44	244	332	692
Xayabuly	117	48	133	2,205	2,504
Vientiane capital	118	18	137	1,319	1,593
Xieng khouang	167	51	66	604	889
Viengchanh	167	71	103	1,541	1,884
Boli khamxay	58	45	66	727	897
Khammoun	94	62	75	507	739
Savannakhet	398	290	281	2,882	3,852
Salavanh	149	133	794	5,329	6,405
Sekong	25	28	129	611	794
Champasak	140	133	180	4,736	5,189
Attapeu	18	42	31	413	505
Total	1,748	1,150	2,878	25,965	31,747

From the Table 1, it was found that the Lao PDR has the total number of 31.75 million animals. The most animal portion was chicken, 25.97 million animals or 81.7% of the total numbers. The next lower portions were pig, cow and buffalo respectively.

Moreover, from the calculation of the energy potential

for biogas production from animal manure, the ability of manure gathering was considered. The percentage of the manure gathering from the total manure of cow, buffalo, pig and chicken were 50%, 50%, 80% and 90%, respectively [3]. The energy potential of biogas production from animal manure was shown in Table 2.

Table 2. The energy potential of biogas production

List	Cow	Buffalo	Pig	Chicken	Total
Amount of animal (million)	1.75	1.12	2.88	25.97	31.75
Weight of manure (kg/animal)	5.44	8	1.47	0.03	
Weight of manure (million-kg/day)	9.5	9.2	4.2	0.76	23.6
Percentage can be gathered (%)	50	50	80	90	
Weight of animal manure production. (million-kg/day)	4.7	4.6	3.3	0.7	13.3
Volume of biogas can be produced (liter/kg)	90	90	340	310	
Volume of biogas production. (million-liter/day)	428	415	1,149	217	2,210
Volume of biogas production. (million-m^3/year)	156	152	419	79	807

From Table 2, it was found that the total of energy from biogas production in the Lao P.D.R was 807 million m^3/year. This was assumed to be able to produce electricity about 1,163 million kWh (1 m^3 of biogas is equivalent to 1.4 kWh). [3] In other case, 1 m^3 of biogas is equivalent to more than 1.4 kWh, which depends on the efficiency of the generator.

The potential of biogas production which was pig's manure has the highest 419 million m^3/year or 52% of the total energy potential. The next highest potential was the manure of cow, buffalo and chicken which had a portion of 19%, 19%, and 11%, respectively. The percentage of volume of biogas was shown in Figure 1.

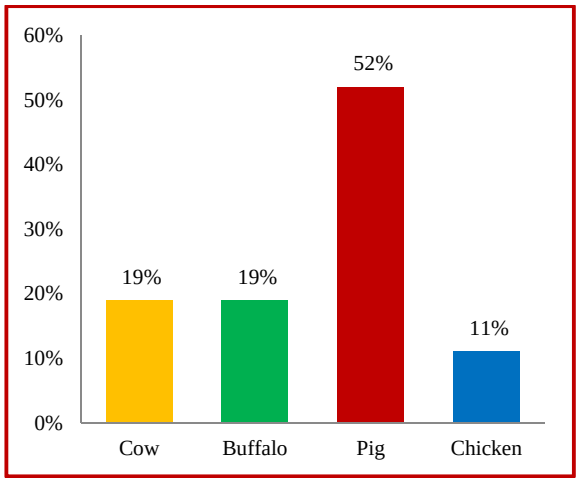

Fig. 1. The percentage of volume of biogas production.

Furthermore, consider the energy potential of biogas production segmented by provinces, it was found that the potential area was divided in to 3 groups as shown in Figure 2.

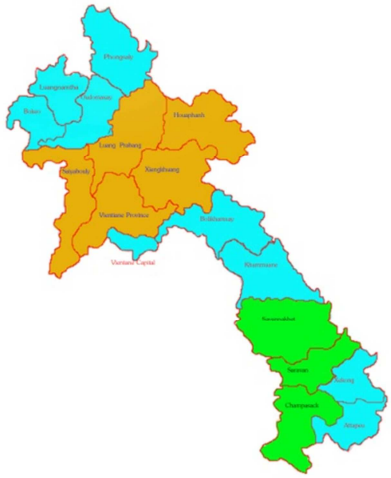

Fig. 2. Map of energy potential of Lao P.D.R.

From Figure 2, three groups were the high potential provinces (Green), the middle potential provinces (Yellow), and low potential provinces (Blue), respectively. The high potential group has an energy potential more than 70 million m^3/year of biogas production. The provinces in this group were Savannakhet, Salavanh and Champasak provinces. The middle potential group has an energy potential of biogas production between 37 to 70 million m^3/year. The low potential group has an energy potential less than 37 million m^3/year of biogas production. The average biogas product for each level was shown in Table 3.

Table 3. The average of energy potential in Lao P.D.R

Rank	Provinces	Amount of animal (10^3 unit)	Biogas production (m^3/year)	Average (m^3/year)
High potential	Savannakhet	3,852	123.51	119.06
	Salavanh	6,405	162.96	
	Champasak	5,189	70.72	
Middle potential	Huaphan	692	48.85	44.03
	Louang phabang	692	47.18	
	Xayabuly	2,504	44.20	
	Vientiane capital	1,593	42.92	
	Xieng khouang	889	37.00	
Low potential	Phongsaly	785	33.51	25.47
	Louang namtha	584	18.36	
	Oudomxay	1,703	34.17	
	Bokeo	542	18.28	
	Viengchanh	1,884	33.19	
	Boli khamxay	897	23.07	
	Khammoun	739	29.07	
	Sekong	794	26.70	
	Attapeu	505	12.95	

4. CASE STUDY

A feasibility of biogas production project was studied by using economic analysis. The pig farm with 520 pigs were selected to use in this study. The basic data of the case study were shown below

1) The farm has the average of electrical consumption of 3,453 kWh/month or 2,689,822 kip/month (1 kWh equivalent to 799 kip)

2) The pig are 520 pigs, which consists of male pig, sow and piglet with the number of 20, 100 and 400, respectively.

4.1 Estimation of Potential Biogas in the Farm

The biogas production potential was calculated and shown in Table 4.

From table 4, it was found that there was 644.60 kg/day and the biogas potential can be produced 175.33m^3/day. This can be able to produce electricity about 245kWh/day.

Table 4. The biogas production potential in the farm

List	Male pig	Sow	Piglet	Total
Amount of pig	20	100	400	31.75
Weight of manure (kg/animal/day)	1.83	1.40	1.17	
Weight of manure (kg/day)	36.60	140.00	468.00	644.60
Percentage can be gathered (%)	80	80	80	
Weight of animal manure production. (kg/day)	29.28	112	374.4	515.68
Volume of biogas can be produced (liter/kg)	340	340	340	
Volume of biogas production. (liter/day)	9,955	38,080	127,296	175,33

4.2 Economic Analysis of the Project

The economic analysis was done and based on the following conditions;

i) Project period is 15 years.

ii) Discount rate is 10%.

iii) Operation days are 365 days.

iv) Technology of Biogas is MC-UASB (Medium Farm Channel Up flow Anaerobic Sludge Blanket) is used [5].

v) The size of biogas system is selected to be 200 m^3.

The project cost for construction of biogas system was shown in Table 5, and the operating cost and return from biogas system were shown in Table 6 and Table 7, respectively.

Table 5. The project cost of building biogas systems.

Investment cost	Amount (kip)
1. Biogas production system	56,348,750
2. Power house	10,355,000
3. Power generator (15 kW)	53,000,000
4. Consultant	53,000,000
5. Transportation	2,000,000
Total	174,703,750

Table 6. The operation and management cost of biogas production system (O&M).

O&M cost	Amount/year (kip)
1. Labour	7,512,000
2. Maintenance of generator	17,490,000
3. Electricity price	3,600,000
Total	28,602,000

Table 7. The returns from biogas system

Volume of biogas production. (m^3/day)	175.33
1m^3 of biogas equivalent to 1.4 kWh	1.4
Energy power (kWh/day)	245
Electricity price (kip/kWh)	779
Total of Amount/year (kip)	70,605,168

From table 5 to table 7, the total project cost for investment of biogas production system was 174,703,750 kip (Lao currency), the operation and management cost was 28,602,000 kip/year, and the returns from biogas system was 70,605,168 kip/year. Thus the net revenue of this project was calculated as below:

Net Revenue = Revenue - Payment (O&M)

= 70,605,168 - 28,602,000

Net Revenue = 42,003,173 kip/year.

4.3 Economic Calculation

The net present value (NPV) can be calculated from investment cost and the present value of benefit (PVB). The PVB means the conversion of all revenue of the project to the revenue in the present as the following the equation;

$$PVB = FV / (1+r)^n \quad (5)$$

$$= \frac{42,003,172}{(1+0.1)^1} + \ldots + \frac{42,003,172}{(1+0.1)^{15}}$$

PVB = 319,479,473 kip

From equation (1), NPV can be calculated by

NPV = PVB− PVC

NPV = 319,479,473 - 174,703,750

NPV = 144,775,723 kip

From the calculation, it was found that the NPV of the project during 15 years was 144,775,723 kip.

The internal rate of return (IRR) can be calculated from investment cost (I) and revenue of project (R) from equation (2) as follows:

$$\frac{42,003,172}{(1+k)^1} + \ldots + \frac{42,003,172}{(1+k)^{15}} = 174,703,750$$

k = 0.2296 or IRR = 22.96 %

From the calculation, it was found that the IRR of the project was 22.96%.

The payback period (PB) can be calculated from equation (3) as follow:

PB = Initial Cost / Net Revenue

PB = 174,703,750 / 42,003,172

PB = 4.16 years

The result has shown that the PB of the project was 4.16 years.

The benefit cost ratio (B/C) can be calculated with comparison the present value of benefit (PVB) and investment cost from equation (4) as follow:

$$B/C = \frac{319,479,473}{174,703,750} = 1.82$$

The result has shown that the B/C of the project was 1.82.

All results of financial analysis can be shown in Table 8.

Table 8. The result of economic analysis of the farm

NPV (kip)	IRR (%)	PB (year)	B/C (kip)
144,775,723	22.96	4.16	1.82

4. CONCLUSION

From the study, the results revealed that the Lao P.D.R has a potential of biogas production from animal manure of 807 million m^3/year or 1,163 million kWh. The result can give important data of biogas production potential to Lao P.D.R for encouraging and developing the alternative energy within the country.

Moreover, from the financial analysis of the case study, it was found that the net present value (NPV) at discount rate (10%) was 144,775,723. It has profit from the investment. The internal rate of return of the project (IRR) was 22.96%, which was more than the discount rate. The payback period was 4.1 years and the benefit cost ratio (BCR) was 1.82. The project of biogas production was acceptable and feasible to promote in Lao PDR.

ACKNOWLEDGMENT

The authors acknowledge the grant from Thailand International Development Cooperation Agency (TICA). The authors are also grateful to acknowledge Farm Engineering and Automation Technology Research Group, Khon Kaen University for supporting a tool and the equipment using in this research.

REFERENCES

[1] Ministry of Energy and Mines. 2011. The Energy Development Strategy of the Lao PDR.

[2] Kamonwan Channee. 2010. A study of biogas production from animal farm Faculty of agriculture Khon Kaen University. Khon Kaen University.
[3] Pattamavadee Sittivoradet and Ratchaphon Suntivarakorn. 2013. An appropriate approach for biogas production and utilization from waste food and animal manure in Khon Kaen University. KKU Engineering Journal. January-March 2013, 40(1):35-46
[4] Ministry of Agriculture and Forestry. Department of Livestock and Fisheries. 2012. Statistics of animal and farming in Lao PDR.
[5] Biogas production systems and wastewater treatment swine model MC-UASB # 1, Biogas Technology, Chiang Mai University. Retrieved August 7, 2013 from World Wide Web: http://teenet.cmu.ac.th/btc/ documents/MC-UASB1.pdf.

Reliability Centered Maintenance (RCM) Implementation on PEA Power Distribution Systems: A Case Study of Bang-Pa-In Branch Office

Watchara Pobporn*, Onurai Noohawm, and Dulpichet Rerkpreedapong

***Abstract*—** *This paper describes a Reliability Centered Maintenance (RCM) implementation on PEA power distribution systems. In order to achieve a cost-effective maintenance program, RCM is to prioritize the failure modes according to their effects, and then to select the effective maintenance activities for those failure modes. Preventive maintenance (PM) activities are mainly focused on the RCM program driven by the marginal benefit-to-cost ratio (B/C) between outage costs and maintenance costs. For a case study, Bang Pa In branch office located in Phra Nakhorn Si Ayutthaya Province, one of local power distribution utilities of Provincial Electricity Authority Central Area 1 (PEA C1) is selected for RCM implementation.*

***Keywords*— Power distribution reliability, maintenance planning, cost-effective maintenance, failure modes.**

1. INTRODUCTION

All industrial units require a reliable production process for sustainable survival in growing competition in today's economy. It is apparent that the continuity of power supply is essential to the function of industrial processes.

Therefore, power distribution systems operated by electric utilities must provide even more reliable electrical power to serve such requirement. This has become the primary objective of electric utilities to maintain their power distribution infrastructure at peak reliability levels.

Reliability Centered Maintenance (RCM) is a method of maintenance optimization widely used in global industries. In this paper, RCM is modified to a simple version well suited for applications to PEA power distribution networks. The main concept of the modified RCM is to prioritize the failure modes according to their effects, and then to select the effective maintenance activities for those failure modes. Preventive maintenance (PM) activities are mainly focused on the RCM program taking into account the marginal benefit-to-cost ratio (B/C) between outage costs (OC) and maintenance costs.

In this paper, the modified RCM is applied to power distribution systems of a PEA local utility, Bang Pa In branch office in Phra Nakhorn Si Ayutthaya Province in Central Area 1 of Provincial Electricity Authority of Thailand (PEA C1). The method is illustrated in step by step procedure. The PM program resulted from the proposed RCM guarantees the cost effectiveness, and reduces the amount of corrective maintenance (CM) and outage costs of both PEA and their customers.

W. Pobporn (corresponding author) is with the Department of Electrical Engineering, Faculty of Engineering, Kasetsart University and with Engineering & Maintenance Division, Provincial Electricity Authority (PEA), Area 1 (Central), Asia Rd., Hantra, Phra Nakhorn Si Ayutthaya 13000, Thailand. Phone: +66-35-241-142 ext. 31413; Fax: +66-35-323-867; E-mail: watcharapob@hotmail.com, watchara.pob@pea.co.th

O. Noohawm and D. Rerkpreedapong are with the Department of Electrical Engineering, Faculty of Engineering, Kasetsart University, 50 Ngamwongwan Rd., Ladyao, Chatuchak, Bangkok, 10900, Thailand. Phone: 66-2-797-9999 ext.1543; E-mail: dulpichet.r@ku.ac.th

2. OVERVIEW OF RCM

Reliability centered maintenance is a qualitative method for determining applicable and effective preventive maintenance tasks to preserve the primary function of selected components or systems. RCM has been widely used in a number of industries since it increases cost effectiveness of maintenance programs, and provides a better understanding of criticality of failure modes that interrupt the system from functioning. The general RCM process [1]-[4] is summarized in the following steps.

1. List the critical components and define their functions

2. Identify the dominant failure modes for each chosen component, and then prioritize the failure mode criticality determined from their failure history and consequences.

3. Determine preventive maintenance tasks for those critical failure modes.

4. Formulate an RCM program.

5. Evaluate the worth of RCM Program including cost analysis.

3. Modified RCM and Case Study

The RCM procedure is modified to a simple version well suited for applications with PEA power distribution networks. It is presented in four steps as follows.

Step 1: Feeder Selection and Information Collection

Step 2: Definition of Feeder Boundary and Function

Step 3: Failure Modes and Effects Analysis

Step 4: Preventive Maintenance Task Selection

The above steps are illustrated through an application

to a case study, which is Bang Pa In branch office. It is one of twenty branch offices in PEA C1, supplying electricity to 35,155 customers. The Bang Pa In branch office is responsible for 8 substations with 441 circuit-km of 22-kV power distribution system. In the case study, the proposed RCM method is applied to 3 critical substations including 26 feeders that supply electrical power to large industrial and commercial customers.

***Step 1*: Feeder Selection and Information Collection.**

The first step of RCM is the selection of power distribution feeders. To do this task, PEA maintenance data must be collected such as technical documents, interruption records, historical maintenance tasks data and maintenance expenses. The interruption records from year 2010 to September 2013 are shown in Table 1. Those interruptions were caused by unknown causes, equipment failures such as fuses, insulators and cable spacers, animals, and lightning strikes.

Table 1. Number of Interruptions by Failure Causes

Failure causes	Substation		
	BKS	BNL	BNM
Equipment failures	10	4	3
Unknown	26	22	6
Birds	1	1	0
Snakes	2	0	0
Lightning strikes	0	0	1

In this step, the interruption records are considered to select a few significant distribution feeders for RCM implementation. They are selected from the outage cost ranking of all feeders of Bang Pa In branch office. Each feeder outage cost is a sum of PEA and customer outage costs as described in equations (1) to (4). As a result, feeders BKS06, BNL01, BNL03 and BKS04 are selected because their outage costs as given in Table 2. are higher than the others as shown in Fig. 1. Then, the single-line diagrams of those feeders are prepared, interruption statistic of selected feeder in the next step.

$$FOC^{i} = \sum_{k} FOC_{k}^{i} = \sum_{k} (OC_{k}^{i,PEA} + OC_{k}^{i,Cust}) \quad (1)$$

$$OC_{k}^{i,PEA} = ICA_{PEA} \times \lambda^{i} \quad (2)$$

$$OC_{k}^{i,Cust} = ICPE_{Cust.} \times \lambda^{i} \quad (3)$$

$$ICA_{PEA} = CM + LossLoad \quad (4)$$

where

FOC^{i} Total outage cost of feeder i (Baht)

$OC_{k}^{i,PEA}$ PEA outage cost of feeder i (Baht)

$OC_{k}^{i,Cust}$ Customer outage cost of feeder i (Baht)

λ^{i} Failure rate of feeder i (events/yr)

ICA_{PEA} Average PEA interruption cost per event (Baht/event)

$ICPE_{Cust}$ Customer interruption cost per event (Baht/event) [9].

CM Average corrective maintenance cost per event (Baht/event).

LossLoad Average revenue losses due to interruptions per event (Baht/event)

k Interruption cause k.

Then, the benefits resulted from mitigating an interruption cause by associated PM is determined from (5).

$$B_{k}^{i} = \eta_{k} \times FOC_{k}^{i} \quad (5)$$

where

B_{k}^{i} Benefits from mitigating interruption cause k by associated PM of feeder i (Baht).

FOC_{k}^{i} Feeder outage cost due to interruption cause k of feeder i (Baht).

η_{k} Effectiveness ratio of PM mitigating interruption causes k.

Table 2. FOC of Selected Feeders

Feeder	Total FOC(Baht)
BKS06	66,094,209.66
BNL01	52,875,367.72
BNL03	46,265,946.76
BKS04	39,656,525.79

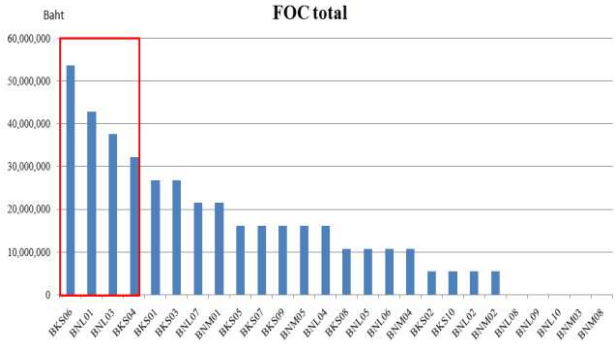

Fig.1. FOC in all feeders.

Step 2: Definition of Feeder Boundary and Function.

In this step, the boundary of all selected feeders is first defined to frame the scope of analysis. It will also help the RCM team members to focus on the targeted areas. In this work, single-line diagrams of the feeders together with geographic maps of service areas of Bang Pa In branch office are used to define the boundaries as shown in Fig. 2 to 4. For each feeder, the boundary covers all medium-voltage equipment. Then, the primary function of each feeder that RCM wishes to preserve is delivering electrical power from the substation to all distribution transformers continuously.

Fig.2. Geographic maps of service areas of Bang Pa In branch office.

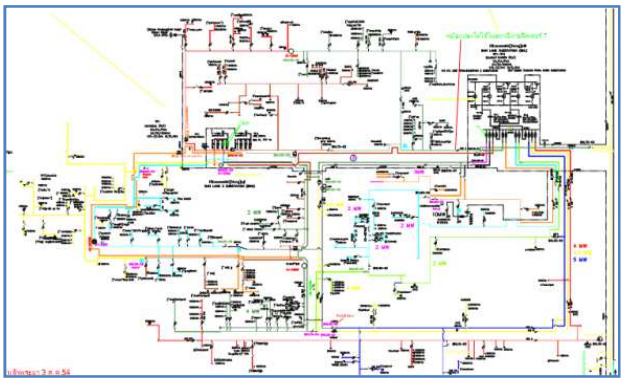

Fig.3. Single line diagram of BNL & BNM substations

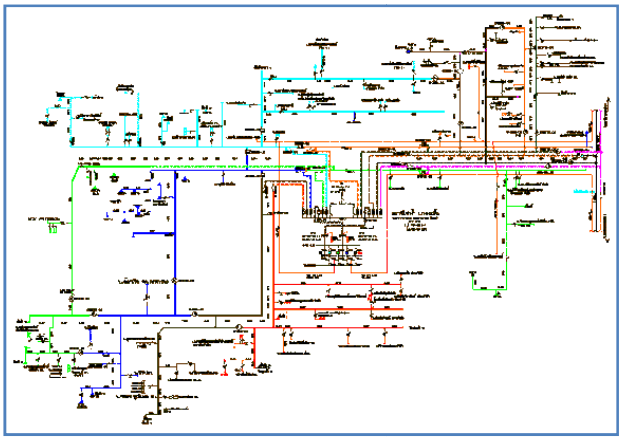

Fig.4. Single line diagram of BKS substations

***Step 3:* Failure modes and Effects Analysis.**

After the primary function of the systems has been specified in the previous step, all dominant failure modes which interrupt the function must be determined. In this paper, the failure mode is defined as the dominant causes that interrupt power delivery. Thus, all failure modes and their effects in terms of FOC are given in Table 2.

Table 2. Feeder failure modes and effects analysis

Feeder	Failure modes	FOC(Baht)
BKS06	Unknown	66,094,210
BNL01	Unknown	39,656,526
	Equipment Failure	13,218,842
BNL03	Unknown	33,047,105
	Equipment Failure	13,218,842
BKS04	Unknown	19,828,263
	Snake	13,218,842
	Bird	6,609,421

***Step 4*: Preventive Maintenance Task Selection**

The objective of this step is to select the optimal PM tasks that achieve the highest reliability worth as presented in terms of a reduction of FOC. In other words, the methodology is designed to find the most cost-effective maintenance tasks. Here, the cost is all expenses of maintenance tasks including hardware costs, labor costs, etc. PM tasks selected for this case study including replacement of bare conductors with spaced aerial cables (SAC), cable spacer maintenance, bird guards or snake guards installation and tree trimming are shown in Table 3. The marginal benefit-to-cost ratio (B/C) between outage costs and maintenance costs is considered to achieve effective PM task selection in equation (5). The costs of maintenance activities are presented in Table 4.

Table 3. Failure modes and associated PM tasks

Failure modes	PM tasks
Unknown	Replacement of bare conductor with SAC
	Cable spacer maintenance
	Bird guard installation
	Snake guard installation
	Tree trimming
Equipment Failures	Replacement of bare conductor with SAC
	Bird guard installation
	Snake guard installation
	Cable spacer maintenance
Snake	Snake guard installation
	Replacement of bare conductor with SAC
Bird	Bird guard installation
	Replacement of bare conductor with SAC

Table 4. Average costs of maintenance activities

Maintenance Task	Average Costs	Unit
Tree trimming	1,083	Baht/km
Snake Guard installation	110	Baht/set
Bird Guard installation	1,000	Baht/set
Replacement of bare conductor with SAC	1,000,000	Baht/cct-km
Cable spacer maintenance	61,700	Baht/km

For example, all PM tasks ranked by marginal benefit-to-cost ratio for BNL01 are shown in Table 5.

Table 5. Ranking of PM tasks for BNL01

Failure modes	PM tasks	B/C
Unknown	Tree trimming	183.16
Unknown	Snake Guard Installation	72.10
Unknown	Bird Guard Installation	38.33
Equipment Failures	Snake Guard Installation	33.65
Equipment Failures	Bird Guard Installation	17.89
Unknown	Cable Spacer maintenance	3.21
Equipment Failures	Cable Spacer maintenance	1.50
Unknown	Replacement of bare conductor with SAC	0.20
Equipment Failures	Replacement of bare conductor with SAC	0.09

For feeder BNL01, the optimal PM tasks which attain the highest marginal B/C ratio are tree trimming, bird guards and snake guards installation and cable spacer maintenance. The marginal benefit-to-cost ratio (B/C) between outage costs and maintenance costs is considered for the effective PM task selection (all dots above red line) for all feeders as shown in Fig. 5 to 8.

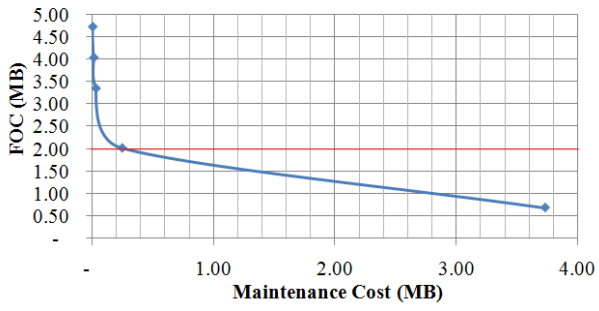

Fig.5. The Maintenance Cost and FOC of BNL01

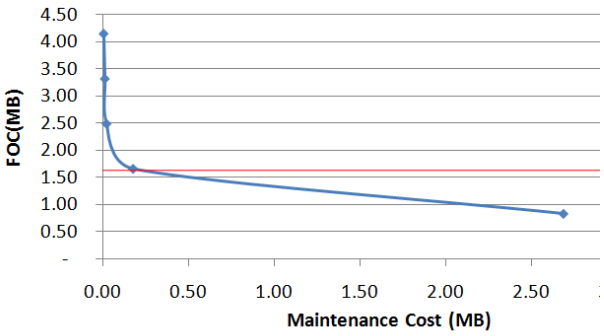

Fig.6. The Maintenance Cost and FOC of BKS06

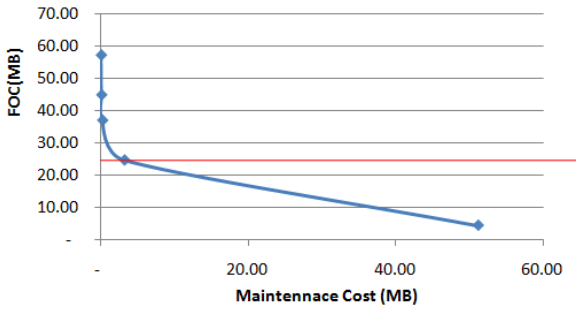

Fig.7. The Maintenance cost and FOC of BNL03

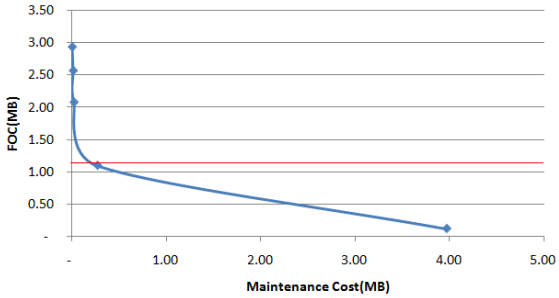

Fig.8. The Maintenance Cost and FOC of BKS04

The total cost of selected PM tasks versus a reduction of feeder outage costs are shown in Table 6. for each feeder.

Table 6. Total cost of PM tasks versus a reduction of FOC

Selected Feeder	Maintenance Cost (Baht)	FOC reduction (Baht)
BKS06	175,774.94	2,488,446.99
BNL01	246,053.28	2,714,092.63
BNL03	3,166,873.10	32,690,592.66
BKS04	270,645.44	1,834,114.32
Total	3,859,346.76	39,727,247

4. CONCLUSION

In this paper, Reliability Centered Maintenance (RCM) is implemented on PEA power distribution systems. In order to achieve a cost-effective maintenance program,

RCM is to prioritize the failure modes according to their effects, and then to select the effective maintenance activities for those failure modes. Preventive maintenance (PM) activities are mainly focused on the RCM program driven by the marginal benefit-to-cost ratio (B/C) between outage costs and maintenance costs. The PM program resulted from the proposed RCM guarantees the cost effectiveness, and reduces the amount of corrective maintenance (CM) and outage costs of both PEA and their customers.

ACKNOWLEDGMENT

The author would like to express his sincere thanks to Kasetsart University, Provincial Electricity Authority Central area1 (PEAC1) and Bang Pa In branch office for the technical data and information of distribution system.

REFERENCES

[1] Aydogan Ozdemir and Elif Deniz Kudasli, RCM Application for Turkish National Power Transmission System, In *Proceedings of IEEE,PMAPS2010*.

[2] Fangxing Li and Richard E. Brown, A Cost-Effective Approach of Prioritizing Distribution Maintenance Based on System Reliability, IEEE transactions on Power Delivery, vol.19, No.1, 2004, pp.439-441.

[3] Lina Bertling, Ron Allan and Roland Eriksson, A Reliability-Centered Asset Maintenance Method for Assessing the Impact of Maintenance in Power Distribution Systems, IEEE transactions on Power Delivery, Vol.20, No.1, 2005, pp.75-82.

[4] A.Sittithumwat, K.Tomsovic and F.Soudi, Optimizing Maintenance Resources in Distribution Systems with Limited Information,

[5] P.Vanittanakom, N.Phoothong, T.Khatsaeng and D.Rerkpreedapong, Reliability Centered Maintenance for PEA Power Distribution Systems. The International Conference on Electrical Engineering, 2008.

[6] Wanda Reder and Dave Flaten, Reliability Centered Maintenance for Distribution Underground Systems,. IEEE transactions on Power Delivery, 2000.

[7] A.Abiri-Jahrommi, M.Fotuhi-Firuzabad and E.Abbasi, An Efficient Mixed-Integer Linear Formulation for Long-Term Overhead Lines Maintenance Scheduling in Power Distribution Systems, IEEE transactions on Power Delivery, Vol.24, No.4, 2009, pp.2043-2053.

[8] Lee Renforth, J.P.White and Robert F. Nelson, The Economic Case for RCM of Overhead lines in the UK, Power Engineering Journal, Oct, 1999.

[9] Thamasart University, PEA project, Customer Outage cost research project progress 4.

On-line Monitoring for Bushing of Power Transformer

Thanapong Suwnansri*, Agkapon Pongmanee, and Cattareeya Suwanasri

Abstract*— *This paper presents the on-line monitoring system for bushing of large power transformer. The system is aimed to detect the degradation of bushing and provides the alarm before bushing failure. Generally the high voltage bushing is produced as a condenser type bushing, consisting of several paper insulation layers separated with conductive foils for each layers. Thus the degradation of internal insulation will affect the value of capacitance and power factor of insulation. These two parameters can be monitored on-line by installing the sensing device at the test tap of bushing. Then the changing of insulation capacitance will lead to the change of leakage current value through bushing insulation. In case of perfect bushing, the leakage current of each bushing should be equal and the summation of all three phase leakage current should be zero. If one bushing has problem with internal insulation, the leakage current will be higher. This makes the summation of current to be greater than zero. This knowledge is used to develop the detection and decision making algorithms in microcontroller and the hardware will be developed to implement as on-line monitoring system for bushing of large power transformer in transmission system.

***Keywords*— Bushing, leakage current, on-line monitoring, power transformer.**

1. INTRODUCTION

Power transformer is one of the key equipment in transmission network. The failure of power transformer is catastrophic that leads to wide area power supply interruption. From the international survey and failure statistics recorded from Thailand transmission system, bushing failure is approximately 20 percent of transformer's failures. The main cause of failure is the aging of seal and gasket due to environmental heat and temperature variation. Moreover, the human error during maintenance can cause the loosen test tap, through which the moisture can pass to the inside insulation of bushing. Thus, the ingress moisture is the main reason of bushing failure.

Therefore, this paper presents the on-line monitoring system for bushing of large power transformer. The system is aimed to detect the degradation of bushing and provides the alarm before bushing failure. Generally the high voltage bushing is made as a condenser type bushing, consisting of several paper insulation layers separated with conductive foils for each layers. Thus the degradation of internal insulation will affect the value of capacitance and power factor of insulation. These two parameters can be monitored on-line by installing the sensing device at the test tap of bushing. Then the changing of insulation capacitance will lead to the change of leakage current value through bushing insulation. In case of perfect bushing, the leakage current of each bushing should be equal and the summation of all three phase leakage current should be zero. If one bushing has problem with internal insulation, the leakage current will be higher. This makes the summation of current to be greater than zero. This knowledge is used to develop the detection and decision making algorithms in microcontroller and the hardware will be developed to implement as on-line monitoring system for bushing of large power transformer in transmission system.

2. CONDENSER BUSHING

Construction

Generally, the bushing of power transformer is made as condenser type, consisting of several paper insulation layers separated with conductive foils for each layers as shown in Fig. 1.

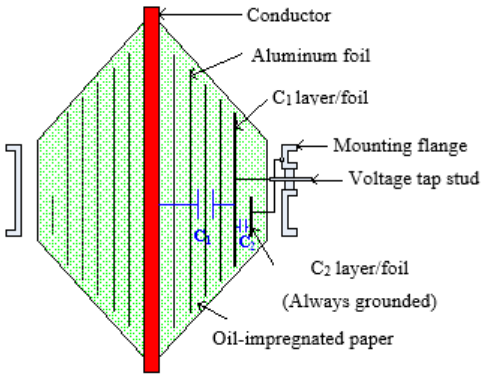

Fig.1. Construction Detail of Typical Condenser Type Bushing.

Assist. Prof. Dr.-Ing. Thanapong Suwanasri (corresponding author) is currently Head of the Electrical and Software System Engineering Department at the Sirindhorn International Thai German Graduate School of Engineering (TGGS), King Mongkut's University of Technology North Bangkok (KMUTNB), 1518 Pracharat 1 Rd, Wongsawang, Bangsue, Bangkok, Thailand 10800. E-mail: thanapongs@kmutnb.ac.th.

Mr. Agkapon Pongmanee is currently a master student at the TGGS, KMUTNB.

Asst. Prof. Dr. Cattareeya Suwanasri is currently the lecturer at Department of Electrical and Computer Engineering, Faculty of Engineering, KMUTNB. E-mail: cattareeyas@kmutnb.ac.th.

The function of conductive aluminum foil in each layer is to obtain the equal voltage distribution in each layer. The space between internal surface of porcelain insulation and condenser set is filled with the insulation oil. Therefore, this condenser type bushing is called as oil impregnated paper or OIP bushing. The high voltage bushing consists of main capacitance C_1 and tap capacitance C_2 as shown in Fig. 2.

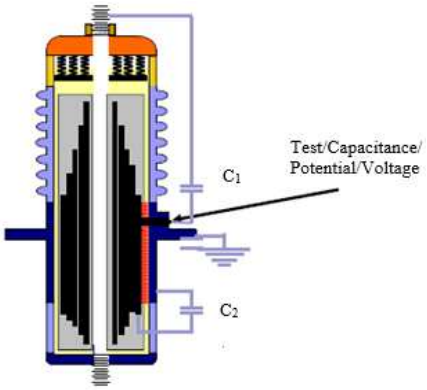

Fig.2. Main Capacitance of Condenser Type Bushing.

Under normal condition, C_1 is connected to ground via voltage tap cover between tap stud and mounting flange, while C_2 is connected to ground without any voltage stress. The degradation of internal insulation will affect the value of capacitance C_1 and power factor of insulation. These two parameters can be monitored on-line by installing the sensing device at the test tap of bushing. C_1 and C_2 will perform as voltage divider and the voltage drop across C_2 can be used with potential device. Then, the changing of insulation capacitance will lead to the change of leakage current value through bushing insulation. In case of perfect bushing, the leakage current of each bushing should be equal and the summation of all three phase leakage current should be zero. If one bushing has problem with internal insulation, the leakage current will be higher. This makes the summation of current to be greater than zero. The summation of three phase leakage current will be compared with the commissioning value or observed the increasing trend in order to set the alarm level. This knowledge is used to develop the detection and decision making algorithms in microcontroller and the hardware will be developed to implement as on-line monitoring system for bushing of large power transformer in transmission system.

Dielectric Loses

Dielectric losses are measured in units of watt loses whereby heat is generated due to these losses. Losses are created by the following causes.

- Natural resistance of the material
- Type of the material
- Polar molecules such as moisture
- Ionization of gases (partial discharge)

Losses will vary by the amount of dielectric material. Since bushing are not the same size and composition, comparison of watt losses between different manufactures, sizes, etc. is difficult. Therefore, the industry uses the power factor to quantify the condition of the bushing insulation system. As loss increases due to any the above causes, the power factor will be also increased. The tap is usually connected to the outer most foil and in some cases to the second to last foil. The C_2 capacitance is the capacitance from the tap to ground. Typically, the tap is grounded; therefore, the C_2 capacitance is not in the circuit during normal operation. Table 1 shows the capacitance of C_1 in bushing of power transformer (Oil-impregnate, paper-insulated type) rated 500 pF, 30.74 V.

Table 1. Capacitance of C_1 in Bushing of Power Transformer Rated 500 pF, 30.74 V

Case	C_1(pF)	ΔC_1	$V_{test\ tap}$ (V)	$\Delta V_{test\ tap}$	Decision
I	500 - 505	1%≤ΔC1	30.74 - 31.05	1%≤ΔC	Normal
II	506 - 515	1%<ΔC1 ≤3%	31.06 - 31.66	1%<ΔC ≤3%	Warning
III	516 - 525	3%<ΔC1 ≤5%	31.67 - 32.28	3%<ΔC ≤5%	Alarm (Low)
IV	526 up	ΔC1>5%	>32.28	ΔC>5%	Alarm (High)

Power Factor

Power Factor (PF) is the phase angle relationship between the applied voltages across a capacitance. The total current through the capacitance is given in Fig. 3.

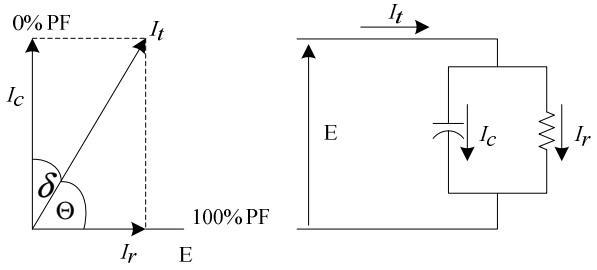

Fig.3. Power Factor Calculating Circuit

For example, power factor can be calculated as follows. Power is equal to Voltage (E) × Current (I_t) × Cosine (θ). Then it is similar to that Watts = E × I_r or Watts = E × I_t × Cosine (θ). Then power factor is calculated as in Eq. (1):

$$PF = Cos(\theta) = \frac{Watts}{E\ x\ I_t} = \frac{E\ x\ I_r}{E\ x\ I_t} = \frac{I_r}{I_t} \quad (1)$$

The variation of power factor should not vary out of the limitation zone (+0.02/-0.04). New bushing condition according to IEEE Std C57.19.01-2000) is given in Fig. 4.

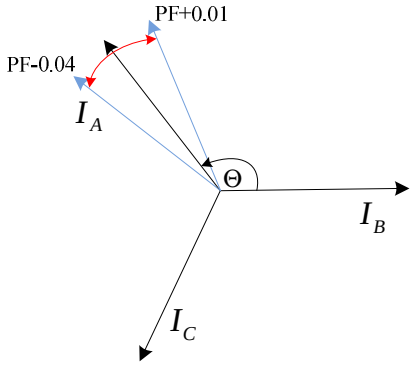

Fig.4. Change in Phase Angle.

3. BASIC THEORY

Bushing On-line Monitoring

In past decades, the off-line monitoring method was used to determine the quality of the bushing insulation. The bushing tests were performed and compared the measured power factor and capacitance to nameplate values or previous tests. Presently, the on-line monitoring method is introduced in order to observe performance of the bushing in real time. Some parameters for both methods are listed as shown in Table 2.

Table 2. Basic Testing Parameter Comparison

Parameters	Off-line Testing	On-line Testing
Applied Voltage	X	
Leakage Current	X	X
Phase Angle between Voltage and Leakage Current	X	
Frequency	X	X

Current Summing

By far, the most common method to monitor bushings is the sum of current method. Fig. 5 shows the installed bushing sensor that use for measure the $V_{test\ tap}$. The concept of measurement has shown in Fig. 6 a block diagram of a bushing monitoring system that uses the sum of currents method. During commissioning the indicator is balanced to zero. The purpose of the balancing circuit is to take into account the differences in system voltages and phase fluctuations and bushing characteristics. As a defect develops the complex conductivity of the bushing insulation changes and the current and its phase angle in one of the phases also changes. Therefore, the indicator will no longer be zero. The amplitude of the change reflects the severity of a problem. Three phase angle indicates in which phase is experiencing the change.

Fig.5. Installed Bushing Sensor.

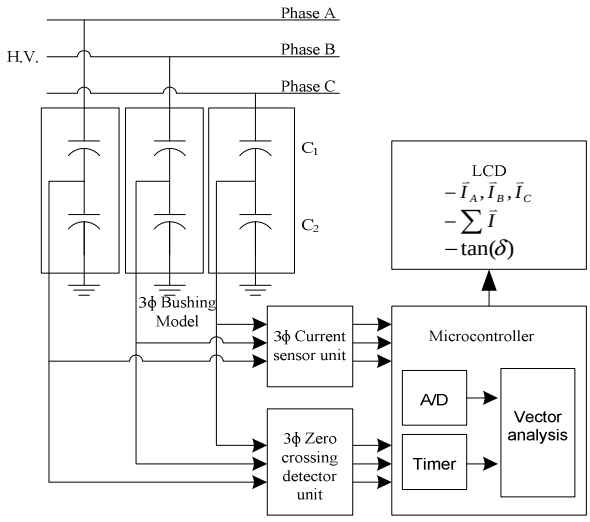

Fig.6. Current Detection from Voltage Tap Circuit.

The change in the sum of currents can be approximately represented by Eq. (2) under the assumption of a single defective phase:

$$\sum I = \frac{\Delta I}{I_0} \approx \sqrt{(\Delta \tan \delta)^2 + \left(\frac{\Delta C_1}{C_1^0}\right)^2} \qquad (2)$$

where:

$\sum I$ - Parameter Sum of Currents

$\Delta \tan \delta$ - Tangent Delta Change,

$\Delta C_1 / C_0$ - Relative Change in Bushing Capacitanc e,

C_0 - Initial Capacitanc e Reading,

I_0 - Initial Sum of Current Value.

Ideally, the sum of the three bushing currents should be zero. In reality, not all parameters are equal from each phase. Therefore during commissioning of the system, the monitor is placed in a balancing mode, and the monitor self-adjusts so the sum of the currents is equal or close to zero.

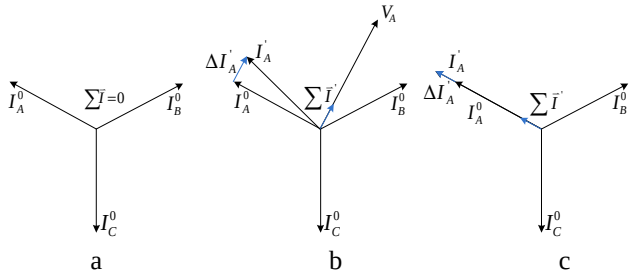

Fig.7. Current Summing Difference Mode.

Figures 7(a), 7(b), and 7(c) explain the method in vector format. Figure 7(a) shows all three currents from the bushing test taps perfectly balanced and the sum equal to zero. If there is a change in tangent delta in the phase-A bushing, an additional active current will pass through the phase-A bushing insulation and the new current I'_A, thus throws the system out of balance. The consequent imbalance vector is equal to the tangent delta change and directed along the phase-A voltage vector in Fig. 7(b). A change in capacitance is shown in Fig. 7(c). This additional current is perpendicular to the phase-A voltage. The consequent imbalance is now positioned along the vector I^0_A.

Voltage Magnitude Trend

The magnitude of the change is an indicator of the problem's severity, and the vector change indicates that bushing is going bad as shown in Fig. 8 whether the power factor or capacitance is changing. The chart and plot shown in Fig. 9 show a recent example of a bushing that is going bad.

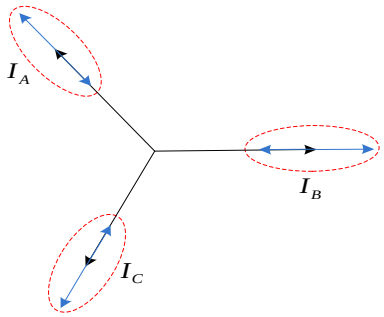

Fig.8. Change in Amplitude

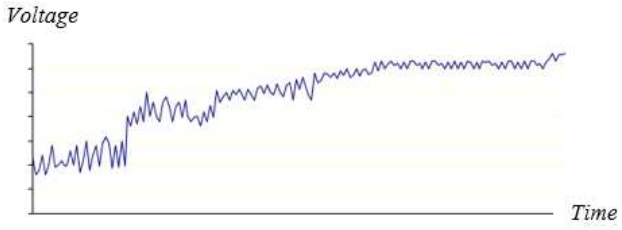

Fig.9. Investigation on Voltage Magnitude Trend

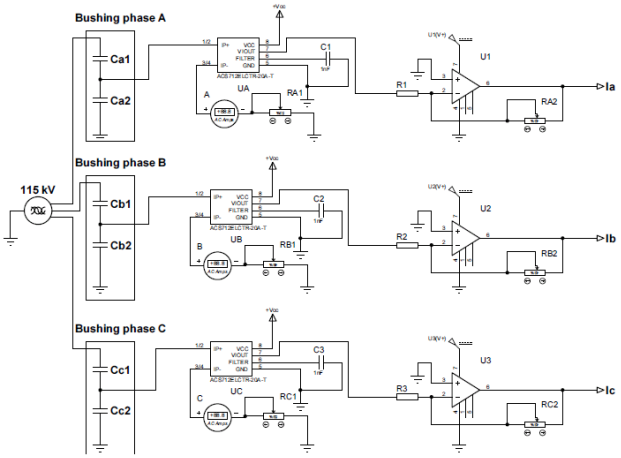

Fig.10. Sensor Circuit

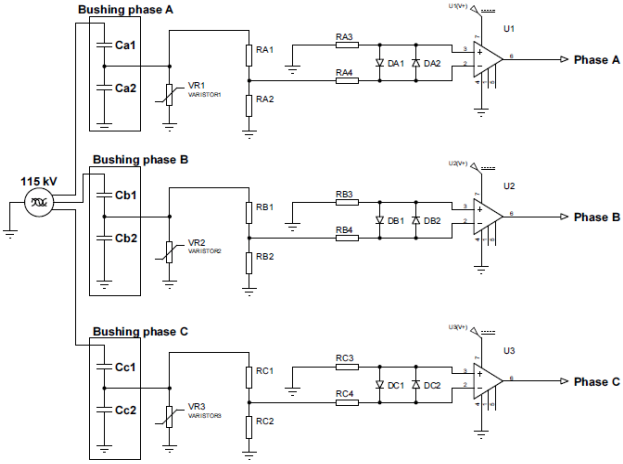

Fig.11. Zero Crossing Detector Circuit

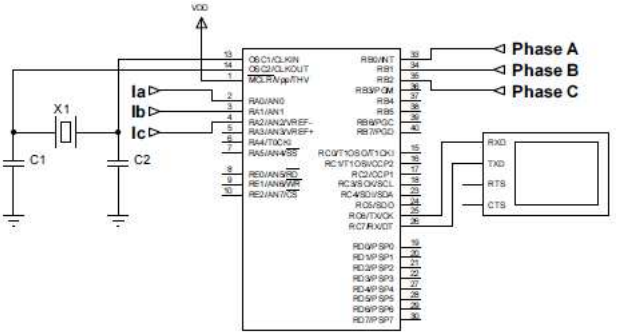

Fig.12. Microcontroller Circuit.

When performing on-line monitoring, the key diagnostic factor is the sum of currents and the phase angle of the sum. Only estimates of the power factor and capacitance can be made since all the data required to calculate the absolute power factor and capacitance is not available, as it is for off line tests. For this reason, on-line bushing monitoring provides relative calculation of power factor and capacitance. When the system goes out of balance, estimates are made on the change of power factor and/or capacitance. Fig. 10 shows the sensor circuit that use to detect the voltage at test tap. The $V_{test\ tap}$ is a key of capacitance measurement. Similarly, the phase angle can be detected via the zero crossing detection technique as shown in Fig. 11. These values are

then added/subtracted to baseline values (nameplate or recent test values) entered into the system. The vector analysis will be calculated by microcontroller as shown in Fig. 12. The microcontroller will get data from both sensor circuit and zero crossing detector circuit and indicate on LCD for help local maintenance know the status of bushing.

If a user has a three phase off-line test set, all the data required is available. For on-line monitoring the following conditions apply:

- The line voltage at the bushing terminals is assumed to be constant on all three phases.
- The phase angles between the phase voltages are constant.
- In additional to the leakage current, the phase angles between Phase A-B and A-C are also measured. The frequency of leakage current is measured from the obtained waveform by performing noise rejection using software filter, performing wave shaping to determine the cycle timing subsequently and recalculating the frequency from known period of one cycle.

4. RESULT AND DISCUSSION

The capacitor testing was done in four different cases. The results are given in Table 3. These four different cases have a same capacitance rating as 500 pF at 30.74 V.

Table 3. Measured Capacitance of C_1 from Measurement System, Rated 500 pF, 30.74 V

Case	C_1(pF)	ΔC_1	$V_{test\ tap}$ (V)	$\Delta V_{test\ tap}$	Decision
I	503	0.60%	30.92	0.60%	Normal
II	509	1.08%	31.29	1.08%	Warning
III	519	3.80%	31.91	3.80%	Alarm (Low)
IV	528	5.60%	32.46	5.60%	Alarm (High)

From the Table 3, the capacitance value of C_1 will directly effect to $V_{test\ tap}$. So, the capacitances changing from 4 cases different are described as bellows.

Case I: The capacitance of C_1 changed from 500 pF to 503 pF mean that the delta capacitance increases to 0.60%. Then it can be concluded that the bushing was in normal condition because the delta capacitance is not more than 1%.

Case II: The capacitance of C_1 changed from 500pF to 509 pF mean that the delta capacitance increases to 1.08%. Then it can be concluded that the bushing was in "warning" condition because the delta capacitance is in length of $1\%<\Delta C_1\leq 3\%$. So the operator should be keep real time monitor.

Case III: The capacitance of C_1 changed from 500pF to 519 pF mean that the delta capacitance increase to3.80%. Then it can be concluded that the bushing was in "Alarm (Low)" condition because the delta capacitance is in length of $3\%<\Delta C_1\leq 5\%$. So the operator should be follow system shutdown procedure and change the new busing into system.

Case IV: The capacitance of C_1 changed from 500 pF to 528 pF mean that the delta capacitance increases to 5.60%. Then it can be concluded that the bushing was in "Alarm (High)" condition because the delta capacitance is more than 5%. So the system will emergency shutdown.

5. CONCLUSION

The diagnostic technique for on-line monitoring of bushing is presented in this work. The degradation of internal insulation will affect the value of capacitance and power factor of insulation. Then the changing of insulation capacitance will lead to the change of leakage current value through bushing insulation. The technique continuously monitors the sum of current in three phases in order to detect the change in value of high voltage capacitance. The sensor circuit and vector analysis in microcontroller has been developed to simulate the degradation of transformer bushing. The status of bushing is indicated in the display as well as warning signal to inform the maintenance officer to correct the problem before bushing failure. The developed system has been tested for several simulation cases and can be further implemented into the hardware for practical application with power transformer in transmission system.

REFERENCES

[1] A. Setayeshmehr, A. Akbari, H. Borsi, E. Gockenbach, "On-line monitoring and diagnoses of power transformer bushings", IEEE Trans. Dielectr. Electr. Insul., vol. 13, no. 3, pp.608-615, June 2006.

[2] *IEEE Standard General Requirements and Test Procedure for Power Apparatus Bushings*, IEEE Standard C57.19.00, 2004.

[3] *IEEE Standard Performance Characteristics and Dimensions for Outdoor Apparatus Bushings*, IEEE Standard C57.19.01, 2000.

[4] M.F. Lachman, W. Walter, P.A. von Guggenberg, "On-line diagnostics of high-voltage bushings and current transformers using the sum current method," IEEE Trans. on Power Del., vol. 15, no. 1, pp.155-162, Jan.2000.

[5] M. Faifer, R. Ottoboni, L. Cristaldi, S. Toscani, "On-line Analysis of Power Transformer Bushings," in *Proc. IEEE Instrumentation and Meaurement Technology Conference*, to be published.

[6] A. Setayeshmehr, A. Akbari, H. Borsi, E. Gockenbach, "On-line monitoring and diagnoses of power transformer bushings", *IEEE Trans. Dielectr. Electr. Insul.*, vol. 13, no. 3, pp.608-615, June 2006.

[7] ABB Power Technology Products AB (2000, Aug. 30). Bushing diagnosis and conditioning - ABB Product information [Online].
Available at:

http://library.abb.com/global/scot/scot252,nsf/veritydisplay/f65a6f910c451bc1c1256bed00302ee3/$File/2750%20515-142%20en%20Rev%200.pdf

[8] Claude Kane, Dynamic Ratings, Inc. On-Line Bushing Monitoring and Comparison To Off-Line Testing. Available at: http://www.dynamicratings.com/US/Application/Transformers/Application%20Notes/AppNote8.pdf

Implementation on LED Road Lighting in Bangkok

Jarin Halapee

Abstract— *This paper presents the study on implementation of a light-emitting diode (LED) luminaire for road lighting in metropolitan area that is been responsible by the Metropolitan Electricity Authority (MEA), Thailand. The LED luminaire were carefully selected in accordance with the MEA and international standards. This is to ensure that such LED luminaire can provide the same value of illuminance as offering by existing luminaires using High Pressure Sodium (HPS) and High-pressure Mercury Vapour (HQV) lamps; but it consumes much lower power. Upon the study, the DIALux program was used to simulate the roadway illumination in several site installations of different landscapes. Various conditions were carefully selected and implemented. The illumination provided by new LED luminaire was then compared against that by the existing luminaires using HPS 250W and HQV 125W lamps. The result shows that the replacement of HPS 250W by LED 140W can reduce power consumption by 169 W/luminaire, which is accounted for 56.5 % reduction. The energy saving can be achieved by 740.22 kWh/luminaire/year, which corresponds to reduction of CO_2 of 0.444 ton/luminaire/year. Furthermore, the replacement of HQV 125W by LED 55W can also reduce power consumption by 92.7 W/luminaire, which is accounted for 64.4 % reduction. As well, the energy saving can be realized by 406.03 kWh/luminaire/year, which corresponds to reduction of CO_2 of 0.243 ton/luminaire/year. Finally, the total energy consumption and cost from the road lighting load can be effectively reduced.*

Keywords— **Road lighting, led road lighting, energy saving lamp.**

1. INTRODUCTION

Presently, a light-emitting diode (LED) technology plays an important role in everyday life; for example in TV monitor, electronic equipment monitor, traffic light, high power torchlight, lighting in building and vehicle as well as road lighting because of its advantages such as low energy conmsumption, longer lifetime, environmental friendliness and so on. It can also be applied to many application according to the user requirement and desiner. Several countries launched LED road lighting project in public area, especially the main significant street in the country. The project applied by LED application is now continuously considered for the future usage [1]. The Metropolitan Electricity Authority (MEA) takes currently consideration on LED technology in the basis of energy conservation in the metropolitan area. Therefore, there is a research project to study, implementation, and installation of LED road lighting in Bangkok [2].

In this paper, the performances of LED luminaire are compared with existing luminaires that are 250W High Pressure Sodium (HPS) and 125W High-pressure Mercury Vapour (HQV) lamps in terms of value of illuminance and energy consumption. The DIALux program was used to simulate the roadway illumination in several site installations of different landscapes. Various conditions based on MEA and international standards [3] were carefully selected and implemented. The illumination provided by new LED luminaire was then compared against that by the existing luminaires using HPS and HQV lamps. The areas in Bangkok taken into the study are Phahurat Road, Chakphet Road and Tri Phet Road, Soi Chidlom, Thetsaban Sai 1 Road.

2. ROAD LIGHTING REQUIREMENT

2.1 MEA Road Lighting Requirement

LED road lighting replacements for existing lamps must be provided illuminance value on roadway according to MEA road lighting requirement [3] by depending on type of roadway as showed in Table 1.

Table 1. Illuminance of MEA Road Lighting Requirement [3]

Road Category	$E_{h\ ave}$ (lux)	U_h
Main Road	15	0.33
Secondary/Local Road (Road width > 6 m)	9.7	0.33
Soi (Road width < 6m)	4.3	0.33
Personal Road	6.5	0.16

$E_{h\ ave}$ = Average value of horizontal illuminance, lux
U_h = Uniformity ratio of horizontal illuminance
$U_h = E_{h\ min} / E_{h\ ave}$

Jarin Halapee was born in Nakhon Si Thammarat, Thailand, in 1976. He received his B.Eng. (E.E.) from King Mongkut's Institute of Technology Ladkrabang (KMITL), Bangkok, Thailand, in 2000. He has joined as an Electrical Engineer with Metropolitan Electricity Authority (MEA) since 2000. At present, he is an Electrical Engineer 8 in Research and Development Department, MEA. His research interests include Overvoltage in Distribution System, Electromagnetic Interference from Power Line, Power Quality and Renewable Energy, Energy saving lamps. E-mail: jarinh@mea.or.th.

2.2 MEA Road Lighting Installation Requirement

Road lighting installation in case of installed on concrete pole and without central reservation for HQV 125W and HPS 250W according to MEA drawing standard [4] based on installation requirement is shown in Table 2.

Table 2. Road Lighting Installation in Case of Installed on Concrete Pole and without Central Reservation

Configuration	HQV 125W	HPS 250W	HPS 250W
Road Width "W" (m)	3 < W < 4	7 < W < 10	10 < W < 13
Luminaire Spacing "S" (MAX.)	32 m	40 m	40 m
Arrangement	Single-Sided Fig.1	Single-Sided Fig.1	Staggered Fig.2
Boom Lenght	1.2 m	1.7 m	1.7 m

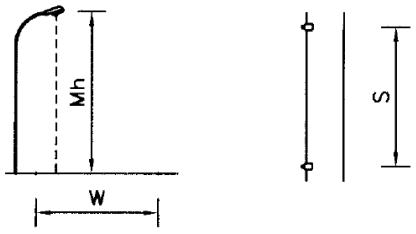

Fig.1. Single-Sided Arrangement

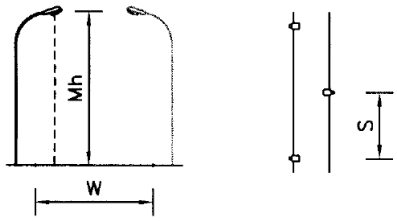

Fig.2. Staggered Arrangement

2.3 Position of Calculation Points

The calculation points according to International Commission on Illumination, CIE 140: 2000 [5] should be evenly spaced in the field of calculation and located as shown in Fig.3.

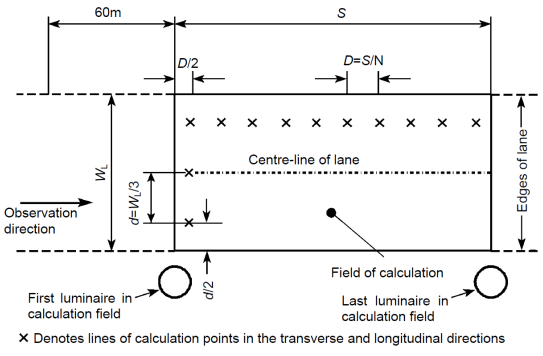

Fig.3. Position of Calculation Points in a Driving Lane.

2.3.1 In the Longitudinal Direction

The spacing (*D*) in the longitudinal direction is determined from the equation (1):

$$D = \frac{S}{N} \quad (1)$$

where: D is the spacing between points in the longitudinal direction (m); S is the spacing between luminaries in the same row (m); N is the number of calculation points in the longitudinal direction chosen such that: for S≤30 m, N=10, for S ≥ 30 m, N is the smallest integer giving D≤3m.

The first transverse row of calculation points is spaced at a distance *D*/2 beyond the first luminaire (remote from the observer).

2.3.2 In the Transverse Direction

The spacing (*d*) in the transverse direction is determined from the equation (2):

$$d = \frac{W_L}{3} \quad (2)$$

where:d is the spacing between points in the transverse direction (m); W_L is the lane width (m).

The outermost calculation points are spaced *d*/2 from the edges of the lane.

3. LED INSTALLATION AND SITE TEST

To compare the illumination performance and the electrical performance according to standard of MEA, HPS 250W with LED 140W, HQV 125W with LED 55W in case of installed on concrete pole and without central reservation was analyzed by using the ideas that include:

- Analysis of illumination performance of HPS and HQV luminaires by installation and measurement data on site test.
- Analysis of illumination performance of LED luminaire by installation and measurement data on site test.
- Analysis of illumination performance of LED luminaire by calculation using DIALux program.

3.1 Condition for Analysis and Site Test

The detail associated with analysis of illumination performance of road lighting has been shown in Table 3.

3.2 Road Lighting Installation Setting for Analysis and Site Test

Site test in the selected site was carried out in MEA distribution area of Samut Prakan province. Three luminaries were set as shown in Fig.4 and Fig.6 and the position of illuminance measurement points as shown in Fig.5 and Fig.7.

Table 3. Detial of Installation and Requirement for Calculation and Testing on Site Test

Luminaire	HPS 250W LED 140W	HQV 125W LED 55W
Arrangment	Single-Sided (Fig.1)	
Road width (m)	8	6
Number of lanes	2	2
Mounting hight (m)	8.5	7.8
Luminaire spacing (m)	40	32(40)*
Overhang (m)	2	1.5
$E_{av\ (@\ MF=0.7)}$ (lux)	15	7.5
U_0 (E_{min}/E_{av})	0.33	0.33

Note:*Luminaire spacing of testing on site test for HQV 125W and LED 55W are 40 m because of limitation of site test.

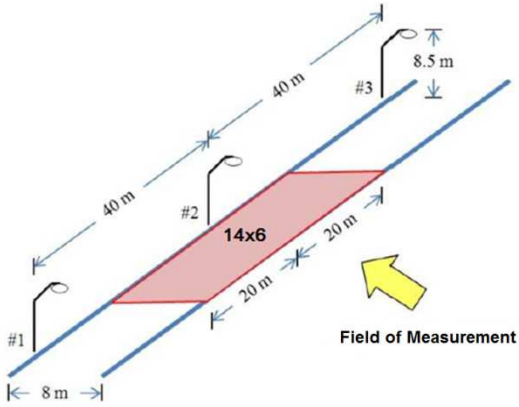

Fig.4. Road Lighting Installation for HPS 250W and LED 140W

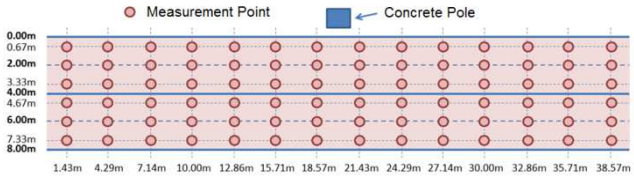

Fig.5. Position of measurement points for HPS 250W and LED 140W

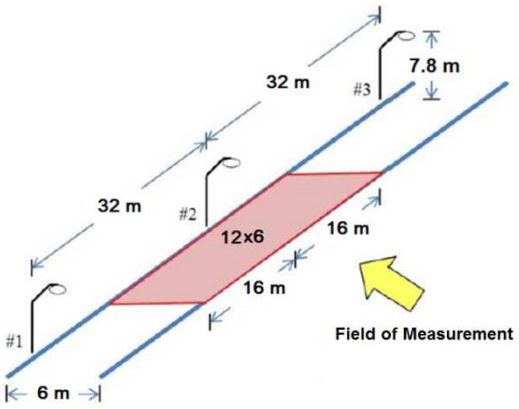

Fig.6. Road Lighting Installation for HQV 125W and LED 55W

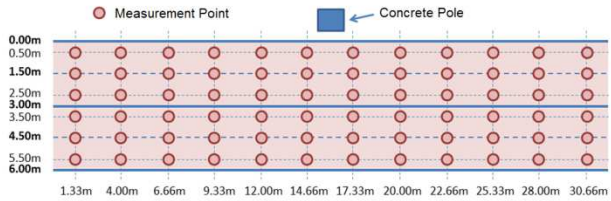

Fig.7. Positions of Measurement for HQV 125W and LED 55W

3.3 Comparative Analysis Result Between HPS 250W and LED 140W

Table 4 shows the comparative analysis result of lighting performance between HPS 250W and LED 140W by following installation and measurement data and using DIALux program on site test with a luminaire spacing as 40 m. Table 5 shows the comparative analysis result of electrical performance between HPS 250W and LED 140W by installation and measurement data on site test. Data was shown as average value per luminaire.

Table 4. Comparison of Lighting Performance between HPS 250W and LED 140W

Parameter	Requirement	HPS 250W	LED 140W
Measurement Result			
$E_{av\ (@\ MF=0.7)}$ (lux)	15	22.07	16.28
U_0 (E_{min}/E_{av})	0.33	0.05	0.29
Calculation Result			
$E_{av\ (@\ MF=0.7)}$ (lux)	15	N/A	14.67
U_0 (E_{min}/E_{av})	0.33	N/A	0.41

Table 5. Comparison of Electrical Performance between HPS 250W and LED 140W (average per luminaire)

Parameter	HPS 250W	LED 140W
Input voltage (V)	230	230
Input current (A)	1.35	0.57
Input power (W)	299	130
Power factor (lag)	0.520	0.985

The results of comparison analysis in Table 4 found that LED 140W had the illumination less than HPS 250W, while providing more than the standard criteriea of MEA, therefore, it can be used replacemented for HPS 250W. Interestingly, comparison in Table 5, LED 140W can reduce the power up to 169 W/luminaire (saving up to 56.5 %).

3.4 Comparative Analysis Result Between HQV 125W and LED 55W

Table 6 shows the comparative analysis result of lighting performance between HQV 125W and LED 55W by following installation and measurement data and using DIALux program on site test with luminaire spacing as 40m and 32m.

Table 7 shows the comparative analysis result of electrical performance between HQV 125W and LED 55W by installation and measurement data on site test. Data was shown as average value per luminaire.

Table 6. Comparison of Lighting Performance between HQV 125W and LED 55W

Parameter	Requirement	HQV 125W	LED 55W
Measurement Result (40 m)			
$E_{av(@MF=0.7)}$ (lux)	7.5	4.12	7.27
U_0 (E_{min}/E_{av})	0.33	0.302	0.151
Calculation Result (40 m)			
$E_{av(@MF=0.7)}$ (lux)	7.5	N/A	6.77
U_0 (E_{min}/E_{av})	0.33	N/A	0.246
Calculation Result (32 m)			
$E_{av(@MF=0.7)}$ (lux)	7.5	N/A	8.39
U_0 (E_{min}/E_{av})	0.33	N/A	0.401

Table 7. Comparison of Electrical Performance between HQV 125W and LED 55W (average per luminaire)

Parameter	HQV 125W	LED 55W
Input voltage (V)	230	230
Input current (A)	1.35	0.23
Input power (W)	144.0	51.3
Power factor (lag)	0.600	0.951

The results of comparison analysis in Table 6 are found that LED 55W had the illumination more than HQV 125W; therefore, it can be concluded that LED 55W can be replaced for HQV 125W. Interestingly, comparison in Table 5, LED 55W can also reduce the power up to 92.7 W/luminaire (saving up to 64.4 %).

4. REPLACEMENT OF EXISTING LAMP BY LED

4.1 Determination on Tested Area

To study and test LED road lighting, the decided areas consist of:

- Phahurat Road, Chakphet Road and Tri Phet Road: replacement of 85 luminaires HPS 250W by LED 140W (Fig.8)
- Soi Chidlom: replacement of 37 luminaires HPS 250W by LED 140W (Fig.9)
- Thetsaban Sai 1 Road: replacement of 20 luminaires HQV 125W by LED 55W (Fig.10)

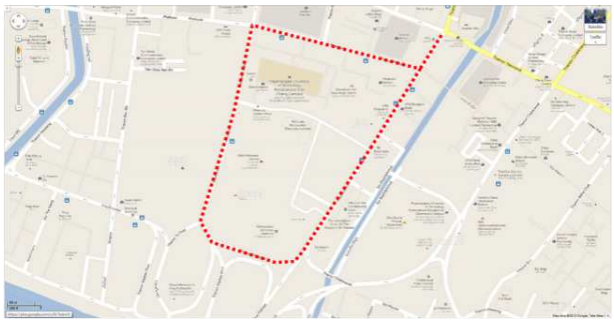

Fig.8. Map of Phahurat Road, Chakphet Road and Tri Phet Road.

Fig.9. Map of Soi Chidlom.

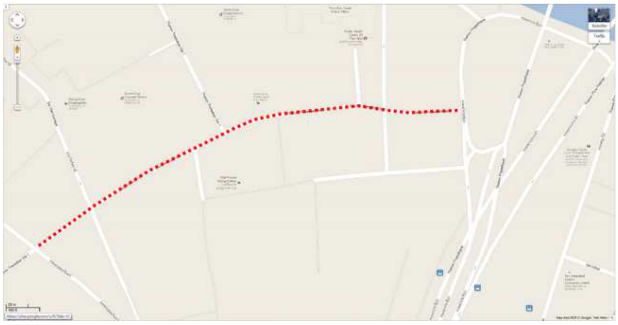

Fig.10. Map of Thetsaban Sai 1 Road.

4.2 Illumination Performances Analysis in Test Areas

Table 9 shows the comparative analysis result of lighting performance between HPS 250W and LED 140W by installation and measurement data on Phahurat Road as shown in Table 8. The results show that although LED 140W provides illumination less than HPS 250W, but it still exceeds the standard criteriea of MEA. Therefore, it can be concluded that the HPS 250W can be replaced by LED 140W.

Table 8. Road Lighting Installation Detail on Phahurat Road

Luminaire	HPS250W/ LED140W
Arrangment	Staggered
Road width (m)	14.5
Number of lanes	5
Mounting hight (m)	8.8
Luminaire spacing (m)	36/32
Overhang (m)	2

Table 9. Comparison of Lighting Performance between HPS 250W and LED 140W on Phahurat Road

Parameter	Requirement	HPS 250W	LED 140W
$E_{av\,(@\,MF=0.7)}$ (lux)	15	37.7	30.7
U_0 (E_{min}/E_{av})	0.33	0.35	0.42

The comparative analysis result of lighting performance between HQV 125W and LED 55W by installation and measurement data on Thetsaban Sai 1 Road as shown in Table 10. It is found that the LED 55W has more illumination than the HQV 125W. Therefore, it can be concluded that the HQV 125W can be replaced by the LED 55W.

Fig.11. Illumination Comparison between HPS 250W (top) and LED 140W (bottom) on Phahurat Road.

Fig.12. Illumination Comparison between HQV 125W (top) and LED 55W (bottom) on Thetsaban Sai 1 Road.

Table 10. Road Lighting Installation Detail on Thetsaban Sai 1 Road

Luminaire	HQV 125W/ LED 55W
Arrangment	Single-Sided
Road width (m)	5
Number of lanes	2
Mounting hight (m)	6.5
Luminaire spacing (m)	33
Overhang (m)	1.5

Table 11. Comparision of Lighting Performance between HQV 125W and LED 55W on Thetsaban Sai 1 Road

Parameter	Requirement	HQV 125W	LED 55W
$E_{av\,(@\,MF=0.7)}$ (lux)	7.5	8.7	15.5
U_0 (E_{min}/E_{av})	0.33	0.25	0.29

4.3 Energy Saving and CO2 Reduction Analysis

Table 12 shows the energy usage by the HPS 250W as compared to replacement by the LED 140W in kWh/luminaire/year. The results show that LED 140W can save energy up to 740.22 kWh/luminaire/year which in turn reduces CO_2 emission by 0.444 ton/luminaire/year. Thus, if one-hundred of LED 140W are installed, the energy will be saved 74,022 kWh/year and can reduce CO_2 emission by 44.413 ton/year.

Table 13 shows the energy usage by the HQV 125W as compared to replacement by the LED 55W in kWh/luminaire/year. The results indicate that using LED 55W can save energy up to 402.03 kWh/luminaire/year which in turn reduces CO_2 emission by 0.243 ton/luminaire/year. Thus, if one-hundred of LED 55W are installed, the energy will be saved 40,603 kWh/year and can reduce CO_2 emission by 24.362 ton/year.

Table 12. Energy Consumption in kWh/luminaire/year of Replacement of Existing HPS 250W by LED 140W

Parameter	HPS 250W	LED 140W
Power Consumption (W)	299	130
kWh/year	299x4,380/1,000 = 1,309.62	130x4,380/1,000 = 569.40
Energy Saving (kWh)	N/A	1,309.62 – 569.40 = 740.22
CO_2 Emission (kg/year)	1,309.62x0.6 = 785.77	569.40x0.6 = 341.64
CO_2 Reduction (kg/year)	N/A	785.77 – 341.64 = 444.13

Note: Average value of CO_2 emissions in Thailand is 563.52 g/kWh or approximate to 0.6 kg/kWh [6]

Table 13. Energy Consumption in kWh/luminaire/year of Replacement of Existing HQV 125W by LED 55W

Parameter	HQV 125W	LED 55W
Power Consumption (W)	144	51.3
kWh/year	144x4,380/1,000 = 630.72	51.3x4,380/1,000 = 224.69
Energy Saving (kWh)	N/A	630.72 – 224.69 = 406.03
CO_2 Emission (kg/year)	630.72x0.6 = 378.43	244.69x0.6 = 134.81
CO_2 Reduction (kg/year)	N/A	378.43 – 143.81 = 243.62

5. ECONOMIC ANALYSIS AND PAYBACK PERIOD

Economic analysis takes into account the energy savings and the cost of the investment of the LED luminaires. Finding a simple payback period can be calculated using the following formula:

$$Payback\ period = \frac{Investment\ cost\ of\ the\ LED\ luminaire}{Evergy\ saving\ cost\ per\ year} \quad (3)$$

The results in Table 14 are found that the payback period for replacement of HPS 250W by LED 140W is 8.57 year and for replacement of HQV 125W by LED 55W is 13.36 year. However, the payback period are depends on energy charge and investment cost.

Table 14. Calculate the simple payback period for this project

Parameter	LED 140W	LED 55W
Energy Saving (kWh/luminaire/year)	740.22	406.03
Energy Charge (THB/kWh)**	3.2532	3.2532
Energy Saving Cost (THB/luminaire/year)	2,408.08	1,320.90
Investment Cost (THB/luminaire)**	20,651.00	17,655.00
Payback Period (year)	8.57	13.36

Note: ** Data in December 2012

6. CONCLUSION

Results associated with the replacement of existing lamp by LED can be summarized as below:

a. LED road lighting 140W can be replaced for HPS 250W. Moreover, LED road lighting 140W can reduce the power up to 169 W/luminaire or might save energy up to 56.6 %.

b. LED 140W replacement for HPS 250W can save energy up to 740.22 kWh/luminaire/year and can reduce CO_2 emission by 0.444 ton/luminaire/year.

c. LED road lighting 55W can be replaced for HQV 125W, Moreover, LED road lighting 55W can reduce the power up to 92.7 W/luminaire or might save energy up to 64.4 %.

d. LED 55W replacement for HQV 125W can save energy up to 406.03 kWh/luminaire/year and can reduce CO_2 emission by 0.243 ton/luminaire/year.

REFERENCES

[1] Metropolitan Electricity Authority; 2011. Final Report: Study on LED Project.

[2] Center of Excellence in Electrical Power Technology, Faculty of Engineering, Chulalongkorn University, 2013. Final Report: Pilot Project for Implementation of LED Road Lighting in Bangkok, proposed Metropolitan Electricity Authority.

[3] Metropolitan Electricity Authority, 2004. DWG. NO. RC-020: Road lighting Requirement.

[4] Metropolitan Electricity Authority, 2008. DWG. NO. 10A4-0646: Road Lighting Arrangement

Depending on Road Width and Selecting Type/Wattage of Lamp.
[5] International Commission on Illumination, 2000. CIE 140: Road Lighting Calculations.
[6] P. Krittayakasem, S. Patumsawad, and S. Garivait, 2001. Emission Inventory of Electricity Generation in Thailand, *Journal of Sustainable Energy & Environment*, 2 (2011), 65 - 69.

Augmented Lagrange Hopfield Network Based Method for Long-Term Hydrothermal Scheduling

Nguyen Trung Thang and Vo Ngoc Dieu*

Abstract*— *This paper proposes an augmented Lagrange Hopfield network (ALHN) based method for solving long-term hydrothermal scheduling problem. The main objective of the problem is to minimize total power generation cost over a scheduling period of one year while satisfying the operating constraints of the hydro and thermal plants, such as the limits on the water storages, discharges, hydro and thermal generations. The ALHN method is a combination of augmented Lagrange relaxation and continuous Hopfield neural network where the augmented Lagrange function is directly used as the energy function of the network. The effectiveness of the proposed method has been tested on two systems and the obtained results compared to those from other methods available in the literature have indicated that the proposed method is very efficient for solving long-term hydrothermal scheduling problem with good optimal solution and fast computational time.

***Keywords*— Long-term hydrothermal scheduling, augmented Lagrange Hopfield network (ALHN), fuel cost function, water storages.**

1. INTRODUCTION

Hydrothermal scheduling is designed to determine a feasible scheduling for power generation in hydro and thermal units that minimizes the operational costs of the system. Since there are many aspects to be considered, including randomness of inflow, hydraulic operational constraints, and electrical transmission constraints, the problem is usually decomposed into a series of long, mid and short-term schedules, with certain aspects represented in each term while others are neglected [1].

The long-term hydrothermal scheduling (LTHTS) problem is concerned with effective utilization of the water inflow to the various hydro reservoirs during the period of interest, usually taken as one year. The solution to this problem consists of the determination of a plant for the withdrawal of water from the hydro reservoirs for power generation throughout the period and the determination of the corresponding thermal generations so that the total cost of fuel is minimized, subject to the operating constraints of the hydro and thermal plants, such as the limits on the water storages, discharges, hydro and thermal power generations [2, 3]. In one of the earlier works [4], the hydrothermal scheduling problem was solved by forming a Lagrange function by augmenting the cost function with the equality constraints on power balance, hydro power generation and the hydro plant characteristic equations. The inequality constraints, namely, limits on water storages, hydro power generations and thermal power generations, are handled by augmenting the cost function with a penalty function. The full problem thus formulated is solved using the conjugate gradient technique. A large computer memory is required in this formulation and the convergence is dependent on the selection of penalty constants [2]. The method of feasible direction [5] was used to solve the hydrothermal scheduling problem. The fundamental principle of this technique is to find a direction of move towards the optimum value. The active constraints are included in determining the direction of move such that it always remains in the feasible domain. An important feature of the approach is its simplicity of formulation as it obviates the need of augmenting the objective function. A local variation algorithm (LVA) [2] has used the method of local variation together with participation factors and the lambda iteration method. The solution approach comprises two phases of computations. In the first phase an initial feasible hydrothermal schedule is obtained and in the second the schedule is improved iteratively to obtain an optimal hydrothermal schedule. Unlike other methods, namely, the conjugate gradient method (CGM) [4] and the feasible direction method (FDM) [5], the proposed method is simple to program, requires the least computer memory and gives an effective optimal solution in reasonable time. Another method based on lambda iteration algorithm and conjugate gradient method to compute discharge (LI-CGM) [6] has reached good quality solutions and certain convergence. J. Sasikala et al. [7] have applied lambda iteration algorithm for solving short term hydrothermal scheduling problem and compare the result from the method with optimal gamma based genetic algorithm. Augmented penalty function method (APFM) [8] has been used to solve LTHTS problem with larger scale than CGM [4] and FDM [5]. The results in terms of fuel cost and computation time have been compared to those from LVA [2]. The

Nguyen trung Thang is with University of Ton Duc Thang, 19 Nguyen Huu Tho str., dist. 7, HCMC, Vietnam. Email: trungthangttt@tdt.edu.vn.

Vo Ngoc Dieu (corresponding author) is with HCMC University of Technology, VNU-HCM, 268 Ly Thuong Kiet str., dist. 10, HCMC, Vietnam. Email: vndieu@gmail.com.

comparison has indicated that APFM [8] is less effective than LVA [2]. The Hopfield neural network (HNN) has been applied to short-term hydrothermal scheduling [9]. There are many drawbacks for such an application. The optimal solution obtained by HNN is sensitive to the selected weighting factors, so selection of the factors is a difficult task. In addition, HNN is very difficult to deal with the complicated problems with nonlinear constraints since the problem constraints have to be linearized before implementing in HNN. Furthermore, for a large-scale system HNN must take long computational time for convergence.

In this paper, a new improvement of continuous Hopfield neural network, called Augmented Lagrange Hopfield network (ALHN) has been proposed for solving long-term hydrothermal scheduling problem. ALHN is a combination of augmented Lagrange relaxation and continuous Hopfield neural network where the augmented Lagrange function is directly used as the energy function of the continuous Hopfield network. On the contrary to HNN, ALHN can obtain the fast convergence for not only simple systems but also large-scale and complicated systems. In order to verify the effectiveness of ALHN two systems are used to perform and the obtained results are compared to those from LVA [2], CGM [4], FDM [5], LI-CGM [6] and APFM [8].

2. PROBLEM FORMULATION

The availability of limited amount of hydroelectric energy, in the form of stored water in the system reservoirs makes the optimal operation complex, because of the link between an operating decision in a given stage and the future consequences of this decision in subsequent stages. Further, it is impossible to have perfect forecasts of the future inflow as well as the load variation during a given period. Therefore, for long term storage regulation, it becomes necessary to account for the random nature of the load and river inflow. A hydrothermal system is considered with N_1 thermal and N_2 hydro plants. The problem is visualized as an M stage decision process by subdividing the planning period into M sub-intervals.

2.1. Thermal fuel cost

The objective function, which is the fuel cost of the thermal plants, is as follows:

$$F_{sm} = a_s + b_s P_{sm} + c_s P_{sm}^2 \tag{1}$$

2.2. Constraints

Load demand

$$P_{Lm} + P_{Dm} - \sum_{s=1}^{N1} P_{sm} - \sum_{h=1}^{N2} P_{hm} = 0 \tag{2}$$

$$P_{Lm} = \sum_{i=1}^{N_1+N_2} \sum_{j=1}^{N_1+N_2} P_{im} B_{ij} P_{jm} + \sum_{i=1}^{N_1+N_2} B_{0i} P_{im} + B_{00} \tag{3}$$

Storage continuity constraint

$$X_{hm} - X_{hm-1} - J_{hm} + q_{hm} = 0, \;\; m = 1, 2, ..., M \tag{4}$$

The limits on the storage level in the reservoirs

$$X_h^{\max} \le X_{hm} \le X_h^{\min} \tag{5}$$

Total volume of water available constraint

$$X_{h0} - X_{hM} + \sum_{m=1}^{M} j_{hm} - \sum_{m=1}^{M} q_{hm} = 0 \tag{6}$$

The limits on water discharge

$$q_h^{\max} \le q_{hm} \le q_h^{\min} \tag{7}$$

Hydro generation

$$P_{hm} = h_{0h}(1 + 0.5e(X_{hm} + X_{hm-1}))(q_{hm} - \rho_h) \tag{8}$$

Generator operating limits

$$P_s^{\min} \le P_{sm} \le P_s^{\max} \tag{9}$$

$$P_h^{\min} \le P_{hm} \le P_h^{\max} \tag{10}$$

3. ALHN BASED METHOD FOR THE PROBLEM

3.1 ALHN for Optimal Solutions

The augmented Lagrange function L of the problem is formulated as follows:

$$\begin{aligned} L = & \sum_{m=1}^{M} T_m \left[\sum_{s=1}^{N1} F_s(P_{sm})\right] + \sum_{m=1}^{M} \lambda_m \left(P_{Lm} + P_{Dm} - \sum_{s=1}^{N1} P_{sm} - \sum_{h=1}^{N2} P_{hm}\right) \\ & + \sum_{h=1}^{N2} \sum_{m=1}^{M} \beta_{hm} (X_{hm} - X_{hm-1} - J_{hm} + q_{hm}) \\ & + \sum_{h=1}^{N2} \sum_{m=1}^{M} \gamma_{hm} \begin{pmatrix} (P_{hm} - h_{0h}(1 + 0.5e(X_{hm} + X_{hm-1})) \\ (q_{hm} - \rho_h) \end{pmatrix} \\ & + \mu_h \sum_{h=1}^{N2} (X_{h0} - X_{hM} + \sum_{m=1}^{M} j_{hm} - \sum_{m=1}^{M} q_{hm}) \\ & + \frac{1}{2} \sum_{m=1}^{M} \beta_{1,m} \left(P_{Lm} + P_{Dm} - \sum_{s=1}^{M} P_{sm} - \sum_{h=1}^{N2} P_{hm}\right)^2 \\ & + \frac{1}{2} \sum_{h=1}^{N2} \sum_{m=1}^{M} \beta_{2,hm} \left(X_{hm} - X_{hm-1} - J_{hm} + q_{hm}\right)^2 \\ & + \frac{1}{2} \sum_{h=1}^{N2} \sum_{m=1}^{M} \beta_{3,hm} \begin{pmatrix} P_{hm} - h_{0h}(1 + 0.5e(X_{hm} + X_{hm-1})) \\ (q_{hm} - \rho_h) \end{pmatrix}^2 \\ & + \frac{1}{2} \beta_{4,h} \sum_{h=1}^{N2} (X_{h0} - X_{hM} + \sum_{m=1}^{M} j_{hm} - \sum_{m=1}^{M} q_{hm})^2 \end{aligned} \tag{11}$$

where λ_m, β_{hm}, μ_h and γ_{hm} are Lagrange multipliers, $\beta_{1,m}$, $\beta_{2,hm}$, $\beta_{3,hm}$ and $\beta_{4,h}$ are penalty factors.

The energy function E of the problem is described in terms of neurons is determined as:

$$
\begin{aligned}
E &= \sum_{m=1}^{M}\sum_{s=1}^{N_1} t_m\left(a_s + b_s V_{p,sm} + c_s V_{p,sm}^2\right) \\
&+ \sum_{m=1}^{M} V_{\lambda,m}(P_{Lm} + P_{Dm} - \sum_{s=1}^{N1} V_{P,sm} - \sum_{h=1}^{N2} V_{P,hm}) \\
&+ \sum_{h=1}^{N2}\sum_{m=1}^{M} V_{\beta,hm}(V_{X,hm} - V_{X,hm-1} - J_{hm} + V_{q,hm}) \\
&+ \sum_{h=1}^{N2}\sum_{m=1}^{M} V_{\gamma,hm}\left\{\begin{matrix} V_{P,hm} - h_{0h}(1 + 0.5e\times \\ (V_{X,hm} + V_{X,hm-1}))(V_{q,hm} - \rho_h) \end{matrix}\right\} \\
&+ V_{\mu h}\sum_{h=1}^{N2}(X_{h0} - X_{hM} + \sum_{m=1}^{M} j_{hm} - \sum_{m=1}^{M} V_{qhm}) \\
&+ \frac{1}{2}\sum_{m=1}^{M}\beta_{1,m}\left(P_{Lm} + P_{Dm} - \sum_{s=1}^{M} V_{P,sm} - \sum_{h=1}^{N2} V_{P,hm}\right)^2 \\
&+ \frac{1}{2}\sum_{h=1}^{N2}\sum_{m=1}^{M}\beta_{2,hm}\left(V_{X,hm} - V_{X,hm-1} - J_{hm} + V_{q,hm}\right)^2 \\
&+ \frac{1}{2}\sum_{h=1}^{N2}\sum_{m=1}^{M}\beta_{3,hm}\left(\begin{matrix} V_{P,hm} - h_{0h}(1 + 0.5e\times \\ (V_{X,hm} + V_{X,hm-1}))(V_{q,hm} - \rho_h) \end{matrix}\right)^2 \\
&+ \frac{1}{2}\beta_{4,h}\sum_{h=1}^{N2}(X_{h0} - X_{hM} + \sum_{m=1}^{M} j_{hm} - \sum_{m=1}^{M} V_{qhm})^2 \\
&+ \sum_{m=1}^{M}\left(\sum_{s=1}^{N_1}\int_0^{V_{P,sm}} g^{-1}(V)dV + \sum_{h=1}^{N_2}\int_0^{V_{P,hm}} g^{-1}(V)dV\right) \\
&+ \sum_{m=1}^{M}\left(\sum_{s=1}^{N_1}\int_0^{V_{X,hm}} g^{-1}(V)dV + \sum_{h=1}^{N_2}\int_0^{V_{q,hm}} g^{-1}(V)dV\right)
\end{aligned} \tag{12}
$$

where $V_{\lambda,m}$, $V_{\beta,hm}$, $V_{\gamma,hm}$ and $V_{\mu,h}$ are the outputs of the multiplier neurons associated with power balance and water constraints, respectively; $V_{P,hm}$, $V_{P,sm}$, $V_{X,hm}$ and $V_{q,hm}$ are the outputs of continuous neurons *hm*, *sm*, *hm* and *hm* representing P_{hm}, P_{sm}, $X_{,hm}$ and q_{hm} respectively.

The dynamics of the model for updating neuron inputs are defined as follows:

$$\frac{dU_{P,sm}}{dt} = -\frac{\partial E}{\partial V_{P,sm}} \tag{13}$$

$$\frac{dU_{P,hm}}{dt} = -\frac{\partial E}{\partial V_{P,hm}} \tag{14}$$

$$\frac{dU_{X,hm}}{dt} = -\left(\frac{\partial E}{\partial V_{X,hm}}\right)_{m\neq M} \tag{15}$$

$$\frac{dU_{q,hm}}{dt} = -\left(\frac{\partial E}{\partial V_{q,hm}}\right)_{m\neq 1} \tag{16}$$

$$\frac{dU_{\lambda m}}{dt} = +\frac{\partial E}{\partial V_{\lambda m}} \tag{17}$$

$$\frac{dU_{\beta hm}}{dt} = +\frac{\partial E}{\partial V_{\beta hm}} \tag{18}$$

$$\frac{dU_{\gamma hm}}{dt} = +\frac{\partial E}{\partial V_{\gamma hm}} \tag{19}$$

$$\frac{dU_{\mu h}}{dt} = +\frac{\partial E}{\partial V_{\mu h}} \tag{20}$$

The inputs of neurons at step *n* are updated:

$$U_{P,sm}^{(n)} = U_{P,sm}^{(n-1)} - \alpha_{P,sm}\frac{\partial E}{\partial V_{P,sm}} \tag{21}$$

$$U_{P,hm}^{(n)} = U_{P,hm}^{(n-1)} - \alpha_{P,hm}\frac{\partial E}{\partial V_{P,hm}} \tag{22}$$

$$U_{X,hm}^{(n)} = U_{X,hm}^{(n-1)} + \alpha_{X,hm}\frac{\partial E}{\partial V_{X,hm}} \tag{23}$$

$$U_{q,hm}^{(n)} = U_{q,hm}^{(n-1)} + \alpha_{q,hm}\frac{\partial E}{\partial V_{q,hm}} \tag{24}$$

$$U_{\lambda,m}^{(n)} = U_{\lambda,m}^{(n-1)} + \alpha_{\lambda,m}\frac{\partial E}{\partial V_{\lambda,m}} \tag{25}$$

$$U_{\gamma,hm}^{(n)} = U_{\gamma,hm}^{(n-1)} + \alpha_{\gamma,hm}\frac{\partial E}{\partial V_{\gamma,hm}} \tag{26}$$

$$U_{\beta,hm}^{(n)} = U_{\beta,hm}^{(n-1)} + \alpha_{\beta,hm}\frac{\partial E}{\partial V_{\beta,hm}} \tag{27}$$

$$U_{\mu,h}^{(n)} = U_{\mu,h}^{(n-1)} + \alpha_{\mu,h}\frac{\partial E}{\partial V_{\mu,h}} \tag{28}$$

where $U_{\lambda,m}$, $U_{\beta,hm}$, $U_{\gamma,hm}$ and $U_{\mu,h}$ are the inputs of the multiplier neurons; $U_{P,hm}$, $U_{P,sm}$, $U_{X,hm}$ and $U_{q,hm}$ are the inputs of continuous neurons. $\alpha_{\lambda,m}$, $\alpha_{\gamma,hm}$, $\alpha_{\beta,hm}$ and $\alpha_{\mu,h}$ are step sizes for updating the inputs of multiplier neurons; and $\alpha_{P,sm}$, $\alpha_{P,hm}$ $\alpha_{X,hm}$ and $\alpha_{q,hm}$ are step sizes for updating the inputs of continuous neurons.

The outputs of continuous neurons and multiplier neurons:

$$V_{P,sm} = \left(P_s^{\max} - P_s^{\min}\right)\left(\frac{1+\tanh(\sigma U_{P,sm})}{2}\right) + P_s^{\min} \tag{29}$$

$$V_{P,hm} = \left(P_h^{\max} - P_h^{\min}\right)\left(\frac{1+\tanh(\sigma U_{P,hm})}{2}\right) + P_h^{\min} \tag{30}$$

$$V_{X,hm} = \left(X_h^{\max} - X_h^{\min}\right)\left(\frac{1+\tanh(\sigma U_{X,hm})}{2}\right) + X_h^{\min} \tag{31}$$

$$V_{q,hm} = \left(q_h^{\max} - q_h^{\min}\right)\left(\frac{1+\tanh(\sigma U_{q,hm})}{2}\right) + q_h^{\min} \tag{32}$$

$$V_{\lambda m} = U_{\lambda m} \tag{33}$$

$$V_{\gamma,hm} = U_{\gamma,hm} \tag{34}$$

$$V_{\beta,hm} = U_{\beta,hm} \tag{35}$$

$$V_{\mu,h} = U_{\mu,h} \tag{36}$$

where σ is slope of sigmoid function that determines the shape of the sigmoid function [10].

3.1.1 Initialization

The initial outputs of continuous neurons are set at their middle limits and the multiplier neurons are set as follows:

$$V_{P,sm}^{(0)} = \left(P_s^{\max} + P_s^{\min}\right)/2 \quad (37)$$

$$V_{P,hm}^{(0)} = \left(P_h^{\max} + P_h^{\min}\right)/2 \quad (38)$$

$$V_{X,hm}^{(0)} = \left(X_h^{\max} + X_h^{\min}\right)/2 \quad (39)$$

$$V_{q,hm}^{(0)} = \left(q_h^{\max} + q_h^{\min}\right)/2 \quad (40)$$

$$V_{\lambda m}^{(0)} = \frac{1}{N_1}\sum_{s=1}^{N_1} \frac{t_{sm}\left(b_s + 2c_s V_{P,sm}^{(0)}\right)}{1 - \dfrac{\partial P_{Lm}}{\partial V_{P,sm}}} \quad (41)$$

$$V_{\gamma h}^{(0)} = \frac{1}{N_2}\sum_{h=1}^{N_2} V_{\lambda m}^{(0)}\left(1 - \frac{\partial P_{Lm}}{\partial V_{P,hm}}\right) \quad (42)$$

$$V_{\beta,h1} = V_{\gamma,m}.h_{0h}\{1 + 0.5e(2V_{X,hm-1} + J_{hm} - 2V_{q,hm}\} \quad (43)$$

$$V_{\beta,hm+1|m\geq 1}^{(0)} = \begin{pmatrix} V_{\beta,hm}^{(0)} - V_{\gamma,hm}^{(0)}\{0.5h_{0h}e(V_{q,hm}^{(0)} - \rho)\} \\ -V_{\gamma,hm+1}^{(0)}\{0.5h_{0h}e(V_{q,hm+1}^{(0)} - \rho)\} \end{pmatrix} \quad (44)$$

3.1.2 Selection of Parameters

By experiment, the value of σ is fixed at 100 for all test systems. The other parameters will vary depending on the data of the considered systems.

3.1.3 Termination Criteria

The algorithm of ALHN will be terminated when either maximum error Err_{max} is lower than a predefined threshold ε or maximum number of iterations N_{max} is reached.

3.1.4 Overall procedure

The overall algorithm of the ALHN for finding an optimal solution for the HTS problem is as follows.

Step 1: Select parameters for the model in Section 3.1.2.

Step 2: Initialize inputs and outputs of all neurons using (37)-(44) as in Section 3.1.1.

Step 3: Set $n = 1$.

Step 4: Calculate dynamics of neurons using (13)-(20).

Step 5: Update inputs of neurons using (21)-(28).

Step 6: Calculate output of neurons using (29)-(36).

Step 7: Calculate errors as in section 3.1.3.

Step 8: If $Err_{max} > \varepsilon$ and $n < N_{max}$, $n = n + 1$ and return to Step 4. Otherwise, stop.

4. NUMERICAL RESULTS

The proposed algorithm has been coded in Matlab 7.2 programming language and executed on an Intel(R) Core (TM)2 Duo CPU T7250 @2.00 GHz PC.

4.1. The first system

The first example chosen consists of a system with two hydro plants and two thermal plants. The incremental costs of the thermal plants are [2, 4]:

$$dF_1/dP_1 = 0.8 + 0.04P_1$$
$$dF_2/dP_2 = 0.78 + 0.06P_2$$

The water inflows in p.u. during the 12 time intervals, the rest of data relating to the expressions for the hydro plants, initial and final storage of the reservoirs and the transmission loss formula matrix are also given in [2, 4]. Load demand for all the time intervals is 8.0p.u. The optimal solutions are given in table 1. Clearly, all generations of each plant for 12 time intervals are the same because of the same load demand of 8.0 pu for all time intervals. The results comparisons in terms of total fuel cost and computation time among ALHN and other methods for the first system are given in the table 2. CGM [4] and FDM [5] have approximate fuel cost and higher than LVA [2] and ALHN. ALHN has the best solution compared to the all ones.

4.2. The second system

The second system has three hydro plants and four thermal plants. The complete data for the second system are from [6, 8]. The optimal solutions from ALHN are given in table 3. The result comparison in terms of total fuel cost and computation time among ALHN and other methods are given in table 4. The cost from ALHN is much less than LI-CGM [6] and APFM [8] but higher than LVA [2].

Clearly, at the both systems, ALHN is much faster than all methods. LVA [2] has been implemented on a 32-bit PRIME 2250 system with 1 MB. There is no computer reported in [4, 5, 6, 8]. Although ALHN has been executed in the better CPU than other methods, computation time of within 2 seconds for each system has also indicated that ALHN is an effective method to solve long term hydrothermal scheduling problem.

Table 1. Optimal solutions using ALHN for the first system.

		Thermal generations		Hydro generations		Water discharge		
m	P_{Dm} (pu)	P_{s1m} (pu)	P_{s2m} (pu)	P_{h1m} (pu)	P_{h2m} (pu)	P_{Lm} (pu)	q_{h1m} (pu)	q_{h2m} (pu)
1	8	2.7288	2.0413	2.2586	1.8843	0.9132	0.7564	1.521
2	8	2.7288	2.0413	2.2586	1.8843	0.9132	0.8227	0.9922
3	8	2.7288	2.0413	2.2586	1.8843	0.9132	0.9969	0.997
4	8	2.7288	2.0413	2.2586	1.8843	0.9132	1.1451	1.5588
5	8	2.7288	2.0413	2.2586	1.8843	0.9132	1.2927	2.4323
6	8	2.7288	2.0413	2.2586	1.8843	0.9132	1.534	2.8734
7	8	2.7288	2.0413	2.2586	1.8843	0.9132	1.6401	2.047
8	8	2.7288	2.0413	2.2586	1.8843	0.9132	1.2486	0.5795
9	8	2.7288	2.0413	2.2586	1.8843	0.9132	0.8853	0.5007
10	8	2.7288	2.0413	2.2586	1.8843	0.9132	0.6376	0.5
11	8	2.7288	2.0413	2.2586	1.8843	0.9132	0.5332	0.5
12	8	2.7288	2.0413	2.2586	1.8843	0.9132	0.5127	0.5

Table 2. Result comparison for the first system

Method	LVA [2]	CGM [4]	FDM [5]	ALHN
Cost ($)	48.6685	48.7512	48.7488	48.5907
CPU time (s)	67	123	102	2.3

Table 3. Optimal solutions using ALHN for the second system

	Thermal generation					Hydro generation			
m	P_{Dm} (MW)	P_{1m} (MW)	P_{2m} (MW)	P_{3m} (MW)	P_{4m} (MW)	P_{1m} (MW)	P_{2m} (MW)	P_{3m} (MW)	P_{Lm} (MW)
1	200	60.8542	50.664	36.334	36.334	13.151	8.0765	0	5.414
2	210	51.6357	42.803	30.5587	30.5587	0.0501	0.2097	61.3109	7.1265
3	205	61.411	51.1399	36.6831	36.6831	6.8325	12.6364	5.1273	5.5145
4	180	50.8341	42.1179	30.053	30.053	9.8902	13.5418	7.3799	3.87
5	195	51.2462	42.4688	30.3113	30.3113	16.0372	17.0841	11.7342	4.1932
6	200	45.7969	37.8322	26.8955	26.8955	25.1512	23.1856	18.2849	4.0417
7	220	43.4586	35.8453	25.4298	25.4298	38.0488	29.0992	27.6018	4.9133
8	204	28.3794	23.0685	15.9782	15.9782	53.7104	33.2545	38.8607	5.2299
9	189	16.3886	12.9543	8.4642	8.4642	66.8045	34.7673	47.4905	6.3328
10	199	18.5544	14.778	9.8211	9.8211	71.4077	33.9512	47.5099	6.8433
11	207	20.38	16.3164	10.965	10.965	75.9744	33.9168	45.7446	7.2622
12	198	13.9493	10.9016	6.9356	6.9356	85.747	33.2368	48.572	8.2771

Table 4. Result comparison for the second system

Method	LVA [2]	LI-CGM [6]	APFM [8]	ALHN
Cost ($)	6234.38	6800.129	6992.73	6777
CPU time (s)	110	-	203	2.2

5. CONCLUSION

In this paper, the proposed Augmented Lagrange Hopfield Network based method is effectively implemented for solving the long-term hydro-thermal scheduling problem. ALHN is a continuous Hopfield neural network with its energy function based on augmented Lagrange function. The ALHN method can find an optimal solution for an optimization in a very fast manner. The effectiveness of the proposed method has been verified through two test systems where the first one consist of two thermal plants and two hydropower plants and the second one has four thermal plants and three hydropower plants. The two systems are scheduled in twelve subintervals. The obtained results compared to those from other methods. The result comparison has indicated that the proposed method can obtain better optimal solutions than other methods. Moreover, the ALHN proposed method also takes the short computation time to get convergence for system ranging from small to larger scale. Therefore, the proposed ALHN method is a promising method for solving long-term hydro-thermal scheduling problem.

NOMENCLATURE

a_s, b_s, c_s	Cost coefficients for thermal unit *s*,
N_1, N_2	Number of thermal and hydro plants.
M	Number of time intervals for scheduling horizon.
P_{Dm}	Load demand of the system during subinterval *m*
P_{hm}	Generation output of hydro unit *h* during subinterval *m*
P_h^{min}, P_h^{max}	Lower and upper generation limits of hydro unit *h*
P_{Lm}	Transmission loss of the system during subinterval *m*
P_{sm}	Generation output of thermal unit *s* during sub-interval *m*
B_{ij}, B_{0i}, B_{00}	Loss formula coefficients of transmission system.
P_s^{min}, P_s^{max}	Lower and upper generation limits of thermal unit *s*
T_m	Duration of subinterval *m*
X_{hm}	Water storage for the *hth* hydro plant during the *mth* sub-interval
J_{hm}	Water inflow into the reservoir for the *hth* hydro plant during the *mth* sub-interval
q_{hm}	Water discharge through the *hth* hydro plant during the *mth* sub-interval
h_{0h}	Basic head of *hth* hydro plant
ρ_h	The non-effective water discharge of the *hth* hydro plant.
e	The water head correction factor to account for variation in head with storage of the *hth* hydro plant.

REFERENCES

[1] G. da Cruz Jr, S. Soares. “Non-Uniform Composite Representation of Hydroelectric Systems for Long-Term Hydrothermal Scheduling” IEEE Proc. Power Industry Computer Application Conference,1995.

[2] M. R. Mohan, K. Kuppusamy and M “Abdullah Khan. “A simple and effective local variation algorithm for long-range hydrothermal scheduling”. Electric Power Systems Research, 24 (1992) 13-18.

[3] B. Türkay , F. Mecitoğlu & S. Baran. “Application of a Fast Evolutionary Algorithm to Short-term Hydro-thermal Generation Scheduling”. Energy Sources, Part B: Economics, Planning, and Policy (2011) 395-405

[4] S. K. Agarwal and I. J. Nagrath, “Optimal scheduling of hydrothermal systems”. Proc. Inst. Electr. Eng., 119 (1972) 169 -173.

[5] T. N. Saha and S. A. Khaparde, “An application of' a direct method to the optimal scheduling of hydrothermal system”. IEEE Trans. PAS-97 (1978) 977-983.

[6] D.P. Kothari and J.S. Dhillon, “Power system optimization”. Second edition. 2011. PHI Leaming Private limited, New Delhi.

[7] J. Sasikala, M. Ramaswamy, “Optimal gamma based fixed head hydrothermal scheduling using genetic algorithm”. Expert Systems with Applications 37 (2010) 3352–3357.

[8] K. S. Prakasa Rao, “Optimal scheduling in hydrothermal power systems by the method of local variations”. Ph.D. Thesis, Indian Inst. Technol., Kanpur. 1974.

[9] M. Basu.“Hopfield neural networks for optimal scheduling of fixed head hydrothermal power systems”. Electr Power Syst Res 2003;64:11–5.

[10] V.N Dieu and W. OngSakul, “Enhanced augmented Lagrangian Hopfield network for unit commitment”, IEE Proc. Gener. Transm. Distrib., vol. 153, no. 6, pp. 624-632, Nov. 2006.

GMSARN International Journal
NOTES FOR AUTHORS

Editorial Policy

In the Greater Mekong Subregion, home to about 250 million people, environmental degradation - including the decline of natural resources and ecosystems will definitely impact on the marginalized groups in society - the poor, the border communities especially women and children and indigenous peoples. The complexity of the challenges are revealed in the current trends in land and forest degradation and desertification, the numerous demands made on the Mekong river - to provide water for industrial and agricultural development, to sustain subsistence fishing, for transport, to maintain delicate ecological and hydrological balance, etc., the widespread loss of biological diversity due to economic activities, climate change and its impacts on the agricultural and river basin systems, and other forms of crises owning to conflicts over access to shared resources. The *GMSARN International Journal* is dedicated to advance knowledge in energy, environment, natural resource management and economical development by the vigorous examination and analysis of theories and good practices, and to encourage innovations needed to establish a successful approach to solve an identified problem.

The *GMSARN International Journal* is a quarterly journal published by GMSARN in March, June, September and December of each year. Papers related to energy, environment, natural resource management, and economical development are published. The papers are reviewed by world renowned referees.

Preparation Guidelines

1. The manuscript should be written in English and the desired of contents is: Title, Author's name, affiliation, and address; Abstract, complete in itself and not exceeding 200 words; Text, divided into sections, each with a separate heading; Acknowledgments; References; and Appendices. The standard International System of Units (SI) should be used.

2. Illustrations (i.e., graphs, charts, drawings, sketches, and diagrams) should be submitted on separate sheets ready for direct reproduction. All illustrations should be numbered consecutively and given proper legends. A list of illustrations should be included in the manuscript. The font of the captions, legends, and other text in the illustrations should be Times New Roman. Legends should use capital letters for the first letter of the first word only and use lower case for the rest of the words. All symbols must be italicized, e.g., α, θ, Q_{wt}. Photographs should be black and white glossy prints; but good color photographs are acceptable.

3. Each reference should be numbered sequentially and these numbers should appear in square brackets in the text, e.g. [1], [2, 3], [4]–[6]. All publications cited in the text should be presented in a list of full references in the Reference section as they appear in the text (not in alphabetical order). Typical examples of references are as follows:

   - **Book references** should contain: name of author(s); year of publication; title; edition; location and publisher. Typical example: [2] Baker, P.R. 1978. Biogas for Cooking Stoves. London: Chapman and Hall.
   - **Journal references** should contains: name of author(s); year of publication; article title; journal name; volume; issue number; and page numbers. For example: Mayer, B.A.; Mitchell, J.W.; and El-Wakil, M.M. 1982. Convective heat transfer in veetrough liner concentrators. Solar Energy 28 (1): 33-40.
   - **Proceedings reference** example: [3] Mayer, A. and Biscaglia, S. 1989. Modelling and analysis of lead acid battery operation. Proceedings of the Ninth EC PV Solar Conference. Reiburg, Germany, 25-29 September. London: Kluwer Academic Publishers.
   - **Technical paper** reference example: [4] Mead, J.V. 1992. Looking at old photographs: Investigating the teacher tales that novice teachers bring with them. Report No. NCRTL-RR-92-4. East Lansing, MI: National Center for Research on Teacher Learning. (ERIC Document Reproduction Service No. ED346082).
   - **Online journal** reference example: [5] Tung, F. Y.-T., and Bowen, S. W. 1998. Targeted inhibition of hepatitis B virus gene expression: A gene therapy approach. Frontiers in Bioscience [On-line serial], 3. Retrieved February 14, 2005 from http://www.bioscience.org/1998/v3/a/tung/a11-15.htm.

4. Manuscript can be uploaded to the website or sent by email to gmsarn@ait.asia. In case of hard copy, three copies of the manuscript should be initially submitted for review. The results of the review along with the referees' comments will be sent to the corresponding author in due course. At the time of final submission, one copy of the manuscript and illustrations (original) should be submitted with the diskette. Please look at the author guide for detail.

GMSARN Members

Asian Institute of Technology

Guangxi University

Hanoi University of Technology

Ho Chi Minh City University of Technology

Institute of Technology of Cambodia

Khon Kaen University

Kunming University of Science and Technology

Nakhon Phanom University

National University of Laos

Royal University of Phnom Penh

Thammasat University

Ubon Ratchathani University

Yangon Technological University

Yunnan University

Associate Member

Mekong River Commission

Published by the

Greater Mekong Subregion Academic and Research Network (GMSARN)
c/o Asian Institute of Technology (AIT)
P.O. Box 4, Klong Luang
Pathumthani 12120, Thailand
Tel: (66-2) 524-6537; Fax: (66-2) 524-6589
E-mail: gmsarn@ait.ac.th
Website: http://www.gmsarn.com